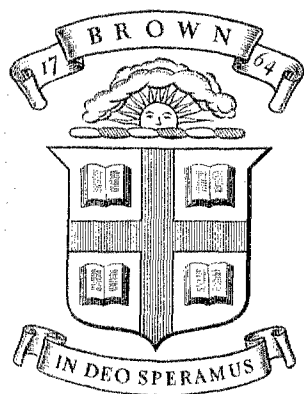


BU
ARPA-E-63



Division of Engineering
BROWN UNIVERSITY
PROVIDENCE, R. I.

STUDIES ON THE DYNAMIC BEHAVIOR
OF RIGID-PLASTIC STRUCTURES

Giuliano Augusti

TECHNICAL LIBRARY
BLDG 313
ABERDEEN PROVING GROUND MD.
BTRAP-TL

AD 685279

Department of Defense
Advanced Research Projects Agency
Contract SD-86
Materials Research Program

ARPA E63

February 1969

BU
ARPA-E-63

I
STUDIES ON THE DYNAMIC BEHAVIOR OF
RIGID-PLASTIC STRUCTURES

by

II
Giuliano Augusti*

III
1. Structures, Rigid
Plastic
2. Loads, Dynamic

Best Available Copy

* Associate Professor of "Scienza delle Costruzioni," Università' di Napoli, Naples, Italy (on leave at the Division of Engineering, Brown University, Providence, Rhode Island)

20040824008




TABLE OF CONTENTS

	<u>Page</u>
INTRODUCTION	1
1. SINGLE-MECHANISM RESPONSE OF A RIGID-PLASTIC STRUCTURE TO DYNAMIC LOADING	3
1.1 Periodic Loading; Case I	4
1.2 Periodic Loading; Case II and "Steady-State" Response	7
2. "MULTI-MECHANISM" RESPONSE AND "SHEAR FRAMES" SUBJECTED TO HORIZONTAL LOADS	12
2.1 "Shear Frames"; Yielding of One Storey	13
2.2 "Shear Frames" with More Storeys Yielding	16
3. THREE-DIMENSIONAL "SHEAR FRAMES" SUBJECTED TO HORIZONTAL LOADS	21
3.1 Static Collapse	22
3.2 Dynamic Behavior	25
4. EFFECTS OF GRAVITY ON THE DYNAMIC BEHAVIOR OF SHEAR FRAMES	35
4.1 Impulsive Load	36
4.2 Periodic Load	38
4.3 Direct Determination of the Critical Cycle n_c Under Periodic Loading	40
SUMMARY AND CONCLUSIONS	45
ACKNOWLEDGMENTS	48
NOTATION	49
REFERENCES	52
LIST AND CAPTIONS OF FIGURES	54

INTRODUCTION

In a number of recent papers, in particular by Martin, Symonds and co-workers [1966-1969] approximate solutions have been sought to the response of plastic structures subjected to dynamic loading, and general theorems for the rational choice and the evaluation of the (average) reliability of such approximations have been established.

However, the applications of these theorems have been mostly limited to impulsive loading problems (i.e. problems in which an initial set of velocities is imposed on the structure). When other loads were allowed to act on the structure, they had to be below the static collapse value [Oien-Martin, 1965].

Only very recently the procedure has been extended to single-pulse loading problems, i.e. problems in which a high load is suddenly imposed on the structure, and then either is suddenly removed after a given time-interval or decays more or less slowly, tending to zero as time increases. (Such sort of loading can be used for instance to approximate blast loading.) It has been shown that a rational approximation, although less satisfactory than for the impulsive loading, is possible in this case also, at least within certain limiting assumptions that may be considered satisfied in most actual instances [Augusti, Martin, O'Keeffe, 1969].

Independently, very similar results were obtained by Kaliszky [1968]* who, however, lacked a general measure of the approximation, although in the several examples in which he compared his approximate results with the exact ones a very good agreement was shown.

* The writer is grateful to Dr. Kaliszky for letting him have an interim copy of the full text of this paper.

As an essential feature of all the works quoted above, the loading program is such that the motion of the rigid-plastic structure lasts only a comparatively short time, after which the structure comes to rest in a permanently deformed configuration. Essentially, no strain reversals take place during the response.

In another important class of dynamic problems, a structure may be subjected to a comparatively large number of repeated and/or reversed loads, as for instance during most strong earthquakes. Problems of this type have been so far treated almost exclusively by numerical means, especially in the plastic range of structural behavior, and no general theorems have been established.

The study of which this report presents the first results, was undertaken with a view of eventually filling this gap and furnishing procedures for the dynamic analysis of plastic structure under any loading history. Therefore, rather than solving particular problems, the attention is focused on recognizing general characteristics, outlining avenues of approach, and so on.

Unfortunately, it has been proved impossible to apply to general loading histories the simple approximate solutions suggested for impulsive and single-pulse loads, while keeping a rational measure of the approximation involved.

A substantial portion of the report deals in particular with periodic loading of structures which behave symmetrically with respect to the sign of the loads; it will be possible to derive some rather general results on the rigid-plastic response in this case, without any qualifications of the structural type. However, the symmetry assumptions are particularly realistic in the case of rectangular frames subjected to horizontal loads, and specific results pertaining to these structures are also presented, including multi-degree of freedom response.

The whole study has so far been limited to rigid-perfectly plastic behavior only: some aspects of this assumption are briefly examined in the Conclusions.

1. SINGLE-MECHANISM RESPONSE OF A RIGID-PLASTIC STRUCTURE TO DYNAMIC LOADING

Consider a rigid-plastic structure, initially at rest, and subjected to variable loads \underline{P}_ℓ , proportional to one time-dependent parameter ξ only:

$$\underline{P}_\ell(t) = \xi(t)\bar{\underline{P}}_\ell \quad (1.01)$$

where $\bar{\underline{P}}_\ell$ is a (fixed) reference value of the ℓ^{th} load (force or couple, concentrated or distributed). For convenience of the following discussion, it will be assumed that $\bar{\underline{P}}_\ell$ has such dimensions that $\xi(t)$ is an acceleration.

Within this definition, the "loading" can be constituted by movements of the external restraints of the structure, in such a way that the distribution of their accelerations is constant with time. In this case, $\xi(t)$ measures directly the acceleration.

Just to fix ideas, consider the very simple example in Fig. 1.1: it is evident that an applied horizontal force $\xi\bar{P}$ and a horizontal ground acceleration $\ddot{u}_g = -\xi$ are equivalent if the reference value is chosen such that $\bar{P} = m$.

This section will deal with the case that the mechanism (i.e. the shape or mode) of the plastic response of the structure is uniquely determined. Therefore, the fields of displacements and strains, of velocities and strain rates, of accelerations and strain accelerations, are also uniquely determined throughout the structure to within a single multiplying factor, which depends on time and can be taken respectively equal to the scalar displacement u , velocity \dot{u} and acceleration \ddot{u} of an arbitrary point of the structure.

Let us indicate by k^+ and $-k^-$ the values of ξ (respectively, positive and negative), corresponding to static collapse of the structure. It is immediate to recognize that the equations of (rigid-plastic) motion of the structure, with the given definitions and assumptions, reduce to

$$\begin{aligned}\ddot{u} &= \xi - k^+ & \text{when } \dot{u} \geq 0 \\ \ddot{u} &= \xi + k^- & \text{when } \dot{u} \leq 0 \\ \ddot{u} &= 0 & \text{when } \dot{u} = 0 \text{ and } -k^- \leq \xi \leq k^+\end{aligned}\tag{1.02}$$

For instance, the motion subsequent to an impulsive loading in the positive- ξ direction* shows a constant deceleration and a linear velocity

$$\ddot{u} = -k^+, \quad \dot{u} = \dot{u}_0 - k^+ t \geq 0\tag{1.03}$$

and a total response time

$$t_f = \frac{\dot{u}_0}{k^+}\tag{1.04}$$

where \dot{u}_0 is the (imposed) initial velocity at $t = 0$. At all times $t \geq t_f$, the third Eq. (1.02) is verified, and the structure remains at rest. If the response mechanism varies in time, the above considerations apply to the "mode approximation" [Martin and Symonds, 1966].

1.1 Periodic Loading; Case I

The assumption of symmetric structural behavior with respect to positive and negative loads implies

$$k^+ = k^- = k\tag{1.05}$$

* In a ξ vs. t diagram, the impulsive load can be represented as a delta function.

It will now be further assumed that the loading is periodic-symmetric, i.e.

$$\xi(t + T) = \xi(t) \quad (1.06)$$

$$\xi(t + \frac{T}{2}) = -\xi(t)$$

where T is the period. An example of loading vs. time diagram of this type is shown in Figs. 1.2a and 1.3a, where the accelerations given by Eqs. (1.02) (for structure initially at rest) are shaded.

In fact, the structure does not yield unless the loading function crosses either of the $\xi = \pm k$ lines. Without lack of generality we can assume that $\xi(t)$ crosses the $\xi = +k$ line first, say at time $t = t_{11}$, and is larger than k for a finite time interval thereafter. According to the previous discussion, the acceleration \ddot{u} is given by the first Eq. (1.02) as long as

$$\dot{u} = \int_{t_{11}}^t \ddot{u} dt \geq 0 \quad (1.07)$$

i.e. for times t comprised in the interval

$$t_{11} \leq t < t_{12} \quad (1.08)$$

where t_{11} has been already defined, and t_{12} is determined by

$$\dot{u}(t_{12}) = \int_{t_{11}}^{t_{12}} \ddot{u} dt = \int_{t_{11}}^{t_{12}} (\xi - k) dt = 0 \quad (1.09)$$

For the simple load-time diagram sketched in Figs. 2a and 3a, Eq. (1.09) implies the equality between the two shaded areas A_{11} and A_{12} .

At time $t = t_{12}$, a discontinuity of \ddot{u} takes place. Either of two conditions can be realized, as exemplified in Figs. 1.2 and 1.3 respectively: namely, either $\xi(t_{12}) \geq -k$ (Fig. 1.2) or $\xi(t_{12}) < -k$ (Fig. 1.3). In the first case, which will be indicated as Case I from now on,

$$\ddot{u}(t) = \dot{u}(t) = 0 \quad \text{for} \quad t_{12} < t \leq t_{13} \quad (1.10)$$

At $t = t_{13}$, determined by

$$\xi(t_{13}) = -k \quad (1.11)$$

or, equivalently, by

$$t_{13} = t_{11} + \frac{T}{2} \quad (1.11')$$

a phase of motion with negative velocity starts, and so on.

A periodic motion with period T is thus activated, as qualitatively illustrated by Fig. 1.2:

$$\begin{aligned} t_{12} - t_{11} = t_{14} - t_{13} = t_{n2} - t_{n1} = t_{n4} - t_{n3} &\leq \frac{T}{2} \\ A_{11} = A_{12} = A_{13} = A_{14} = A_{n1} = A_{n2} = A_{n3} = A_{n4} &= \max|\dot{u}| \\ (n = 1, 2, 3, \dots) \end{aligned} \quad (1.12)$$

The displacement u (periodic but not symmetric) varies between 0 and a positive value Δu , equal to the area of each of the \dot{u} -pulses:

$$0 \leq u(t) \leq \Delta u = \int_{t_{n1}}^{t_{n2}} \dot{u} \, dt = - \int_{t_{n3}}^{t_{n4}} \dot{u} \, dt \quad (1.13)$$

It is of interest to note that the total dissipated plastic work (which could cause failure of the structure because of large-strain fatigue) is proportional to the accumulated absolute values of the displacements*. Then ,

* By assumption, the mechanism is unique; therefore the strain-vectors do not change direction during the motion. When they change sign, the associated stress points jump to points symmetrical with respect to the origin of the stress axes, which by assumption is a center of symmetry for the yield surface. It will be seen in Section 3 that this behavior implies that each stress point is on a principal direction of the relevant yield surface.

after n cycles, the dissipated plastic work is given, to within a positive factor, by

$$\bar{u} = 2n\Delta u \quad (1.14)$$

Therefore, Δu measures both the maximum absolute displacement and the plastic work dissipated in each cycle.

1.2 Periodic Loading; Case II and "Steady State" Response

On the contrary, if

$$\xi(t_{12}) < -k \quad (1.15)$$

the case of Fig. 1.3 is verified, which will be indicated as Case II in the following. The initial instant of the first negative-velocity phase, t_{13} , coincides with the final instant of the first positive-velocity phase, t_{12} :

$$t_{12} = t_{13} > t_{11} + \frac{T}{2} ; \quad (1.15')$$

the acceleration is given by the second Eq. (1.03) for

$$t_{13} < t < t_{14} = t_{21} \quad (1.16)$$

where t_{14} is defined by

$$\dot{u}(t_{14}) = \int_{t_{12}}^{t_{14}} \ddot{u} dt = \int_{t_{12}}^{t_{14}} (\xi + k) dt = 0 \quad (1.17)$$

(i.e., in the simple example in Fig. 1.3a, by the equality of the areas A_{13} and A_{14}) and t_{21} is the starting time for the second cycle of motion.

It can be proved that, provided $k > 0$,

$$t_{21} - t_{11} > T, \text{ i.e. } \xi(t_{21}) > k ; \quad (1.18)$$

therefore, beyond t_{21} , the acceleration is again given by the first Eq. (1.02) and the motion continues as sketched in Fig. 1.3.

The following inequalities can also be easily proved (the relevant quantities being defined in Fig. 1.3a, b, c, all as positive quantities):

$$\begin{aligned} A_{11} &> A_{21} > \dots > A_{n1} > \dots \\ A_{13} &< A_{23} < \dots < A_{n3} < \dots \end{aligned} \quad (1.19)$$

$$A_{21} > A_{13} ; \dots ; A_{n1} > A_{(n-1)3}$$

$$\begin{aligned} \Delta u_{11} &> \Delta u_{21} > \dots > \Delta u_{n1} > \dots \\ \Delta u_{12} &< \Delta u_{22} < \dots < \Delta u_{n2} < \dots \end{aligned} \quad (1.20)$$

$$\Delta u_{21} > \Delta u_{12} ; \dots ; \Delta u_{n1} > \Delta u_{(n-1)2}$$

It is then intuitive that the motion $u(t)$ tends to a periodic motion $u^S(t)$ with

$$A^S = \lim_{n \rightarrow \infty} A_{n1} = \lim_{n \rightarrow \infty} A_{n3} \quad (1.21)$$

$$\Delta u^S = \lim_{n \rightarrow \infty} \Delta u_{n1} = \lim_{n \rightarrow \infty} \Delta u_{n2}$$

In order to demonstrate this intuitive result, consider the situation in Fig. 1.4. The loading diagram $\xi(t)$ and the value of k are the same as in Fig. 1.3, but initial values of acceleration \ddot{u}_0 and velocity \dot{u}_0 have been assumed as follows.

The values of

$$t_{11}^* ; t_{12}^* = t_{11}^* + \frac{T}{2} ; t_{21}^* = t_{11}^* + T ; \text{ etc.} \quad (1.22)$$

have been determined first from the condition

$$A_{11}^* = A_{12}^* = A_{13}^* = A_{14}^* = \dots = A_{n1}^* = A_{n2}^* = A_{n3}^* = A_{n4}^* \quad (1.22')$$

Then \ddot{u}_0 and \dot{u}_0 have been assumed

$$\begin{aligned} \ddot{u}_0 &= -k \\ \dot{u}_0 &= - \int_0^{t_{11}^*} (\xi + k) dt \end{aligned} \quad (1.23)$$

so that

$$\dot{u}(t_{11}^*) = 0 \quad (1.24)$$

The ensuing motion $u(t)$, shown in Fig. 1.4, is periodic. The initial displacement u_0 is arbitrary; in Fig. 1.4c it has been chosen such that $u_{\min} = 0$, so that

$$0 \leq u(t) \leq \Delta u^* = \int_{t_{n1}^*}^{t_{n2}^*} \dot{u} dt \quad (1.25)$$

similar to (1.13).

The two motions in Figs. 1.3 and 1.4 correspond to the same loading and different initial conditions. Therefore, according to Martin's uniqueness theorem [1966], their velocities tend to each other as time increases. In other words, the actual motion $u(t)$ tends to a periodic motion $u^s(t)$ that can be determined as in Fig. 1.4 to within an additive constant, u_{\min} ; A^s and Δu^s in Eqs. (1.21) are given by

$$\begin{aligned} A^s &= A_{n1}^* = A_{n2}^* \\ \Delta u^s &= \Delta u^* \end{aligned} \quad (1.26)$$

The motion $u^s(t)$ will be indicated as the steady state motion (or response); the actual (limit) value of u_{\min} as the final residual displacement u_R .

Note that the rapidity of convergence of $u(t)$ to $u^S(t)$, for a given load-time diagram, decreases with decreasing k . In the limit, if $k = 0$, a motion with a periodic (but not symmetric) velocity and unbounded displacements is activated from the first cycle*.

After a sufficiently large number of cycles the large strain fatigue can be computed on the periodic motion with good approximation

$$\bar{u}(n) \approx 2n\Delta u^* \quad (1.27)$$

The residual displacement after n cycles u_{Rn} is given by (Fig. 1.4)

$$u_{Rn} = \sum_{i=1}^n (\Delta u_{i1} - \Delta u_{i2}) < n(\Delta u_{11} - \Delta u_{12}) \quad (1.28)$$

The total displacement during the n^{th} cycle is limited by

$$u_{R(n-1)} \leq u(t) \leq u_{R(n-1)} + \Delta u_{n1} \quad (t_{n1} \leq t \leq t_{n4}) \quad (1.29)$$

After a sufficiently large number of cycles, Eq. (1.29) is well approximated by

$$u_R \leq u \leq u_R + \Delta u^* \quad (1.29')$$

where the final residual displacement u_R is the limit

$$u_R = \lim_{n \rightarrow \infty} u_{Rn} = \sum_{i=1}^{\infty} (\Delta u_{i1} - \Delta u_{i2}) \quad (1.30)$$

Finally, note that if in Figs. 1.2, 1.3, 1.4 the sign of the ξ -diagrams is changed, the signs (and the signs only) of the \dot{u} and u diagrams change also.

In conclusion, the response of a rigid-plastic structure, under assumptions (1.05) and (1.06), is (or tends to) a periodic motion of finite amplitude and

* One cycle of such a response is illustrated in Fig. 4.7 at the end of the report.

the same period as the forcing function $\xi(t)$. At each instant in which \dot{u} becomes zero, there is a discontinuity $\delta\ddot{u}$ of the acceleration,

$$-2k \leq \delta\ddot{u} \leq 2k \quad (1.31)$$

There is no resonance effect: the characteristics of the response are monotonic functions of the characteristics of the load input.

It is possible to generalize the previous results to periodic but not symmetric loading (only the first of Eqs. (1.06) holds) and/or non-symmetric structural behavior ($k^+ \neq k^-$) . In these cases, a permanent displacement is added in each loading cycle, and the response is equal (or tends) to a motion sum of a periodic plus a linear term. This behavior will not be investigated further, although in Section 4 a sort of induced asymmetry of structural strength will be considered.

2. "MULTI-MECHANISM" RESPONSE AND "SHEAR FRAMES" SUBJECTED TO HORIZONTAL LOADS

All the results in Section 1 were obtained in the assumption that the mechanism (i.e. the "shape" of the deformation field) did not change in time, although some of them (and in particular the periodicity of the steady state response to periodic loading) are indeed valid also if this assumption is lifted.

In the latter case, graphical operations essentially analogous to those illustrated in Figs. 1.2, 1.3 and 1.4 would give the actual and the periodic response. However, the accelerations corresponding to the different degrees of freedom are given by relations rather more complicated than Eqs. (1.02) and different in the different instances, so to make a general discussion very involved if not impossible.

In fact, the departure of the response from the simple single-mechanism type can take place in so many ways that a unique formulation does not seem possible.

To illustrate this point, it is sufficient to consider a uniform simply-supported beam of limit moment M_0 , once loaded by a uniform dynamic load $\xi(t)\bar{q}$ (Fig. 2.1a) and once loaded by a central concentrated force $\xi(t)\bar{P}$ (Fig. 2.1f). In the first case, as long as $k < \xi \leq 3k$, the acceleration and moment diagrams look like in Figs. 2.1b and 2.1c respectively; but as soon as $\xi > 3k$, the central plastic hinge spreads into a plastic zone of finite length Δl , the acceleration (not velocity!) and moment diagrams becoming qualitatively as shown in Figs. 2.1d and 2.1e respectively. In the case of Fig. 2.1f, at first the acceleration diagram looks again like in Fig. 2.1g; successive stages (I, II, III) of the bending moment diagram are illustrated in Fig. 2.1h. At a certain value of ξ , the minimum (max. negative) moment M^* reaches the negative

limit moment $-M_0$, and new plastic hinges are formed: further acceleration and moment diagrams look like in Figs. 2.1i and 2.1j.

Therefore, instead of attempting a general discussion of the multi-degree-of-freedom dynamic rigid-plastic behavior, the present section deals with a specific structural type and loading, namely rectangular multi-storey shear frames subjected to horizontal ground motion (as shown in Fig. 2.2), for which the symmetry conditions (1.05-06) are verified and particularly relevant, and moreover the motions of the several degrees of freedom are determined by remarkably simple relationships.

The following discussion, interesting in itself as the solution of an important structural problem, is also useful as an illustration of the techniques which could be employed for other analogous problems.

The behavior of the multi-storey shear frame can be assimilated to that of the simple-supported beam in Fig. 2.1f, in that a second degree of freedom is activated by formation of new plastic zones (or plastic hinges), while in the beam of Fig. 2.1a the shape of the deformation fields is altered by the spreading of the plastic zone. Another possibility, substantially different from both instances in Fig. 2.1, will be illustrated in Section 3.

2.1 "Shear Frames"; Yielding of One Storey

We define by shear frame a rectangular multi-storey frame such that, under horizontal loads acting on the beams, the plastic hinges form in the top and bottom sections of the columns. The rigid-plastic deformations of such a frame are fully specified by N independent variables u_i , where u_i is the rightward displacement of the i^{th} floor with respect to the $(i-1)^{\text{th}}$ and N the number of storeys (Fig. 2.2).

The shear strength of the i^{th} storey

$$V_{oi} = 2 \frac{\sum_{j=1}^{J_i} M_{oj}}{h_i} \quad (2.01)$$

is supposed known (and equal in both directions), while the number of columns J_i is irrelevant, and can indeed vary from one storey to another, as the other quantities on the right side of Eq. (2.01). Only plane frames are studied in this section, while three-dimensional shear frames will form the object of Section 3.

The frame will be assumed to be subjected to a horizontal ground movement whose acceleration

$$\ddot{u}_g = -\xi(t) \quad (2.02)$$

is a known function of time.

The mass of the i^{th} floor is m_i , and the mass of the columns is negligible in comparison. Then the equivalent loading on the frame is constituted by a set of horizontal forces $m_i \xi$ acting at each floor level, and the total inertia forces are*

$$F_i = m_i (\xi - \sum_{j=1}^i \ddot{u}_j) \quad (2.03)$$

The total shear at the i^{th} storey is given by

$$V_i = \sum_{\ell=1}^N F_{\ell} = \sum_{\ell=1}^N [m_{\ell} (\xi - \sum_{j=1}^{\ell} \ddot{u}_j)] \quad (2.04)$$

Let us assume that at a certain instant the i^{th} storey, but none above it, is deforming plastically, with a positive velocity \dot{u}_i , i.e.

* Cf. the simplest particular case in Fig. 1.1.

$$\sum_{j=1}^{\ell} \ddot{u}_j = \sum_{j=1}^i \ddot{u}_j \quad \text{for } \ell \geq i$$

$$V_i = V_{oi} \quad (2.05)$$

$$0 < V < V_{ol} \quad \text{for } \ell \geq i$$

Because of (2.01) and (2.04), Eqs. (2.05) implies

$$\frac{V_{oi}}{\sum_{j=1}^N m_j} < \frac{V_{ol}}{\sum_{j=1}^N m_j} \quad (\ell \geq i) \quad (2.06)$$

This relation, which is independent of the ground acceleration $-\xi$ and of time t , shows that plastic yielding starts in the p^{th} storey, defined by

$$k_p = \frac{V_{op}}{\sum_{j=1}^N m_j} = \min \left[\frac{V_{oi}}{\sum_{j=1}^N m_j} \right] \quad (i = 1, 2, \dots, N) \quad (2.07)$$

and cannot move upwards along the frame. And if (2.07) is satisfied by $p = 1$ (i.e. by the first or ground storey), as it is very likely to be in an actual frame, then the motion of the (rigid-plastic) frame involves only one degree of freedom: the results of Section 1 apply in full and no further discussion is necessary for such a frame.

It is worthwhile to note that this condition can be verified just because, at every storey except the first, there are infilling walls and other non-structural components which increase the actual shear resistance V_{oi} .

Although the considerations above have been formulated with reference to a specific load condition, they do remain valid for other horizontal loads under not too restrictive assumptions, as long as the definition of "shear frame" holds. In conclusion, the response of a rigid-plastic building frame to horizontal loads

is very likely to involve yielding of the first storey only: use of this conclusion as a greatly simplifying assumption will be of enormous help in the study of other aspects of rigid-plastic frame behavior in later sections of this report.

2.2 "Shear Frames" with More Storeys Yielding

Consider now the case in which Eq. (2.07) is satisfied by $p > 1$. This p^{th} storey yields as soon as $\xi(t)$ crosses either of the lines $\xi = \pm k_p$; again it can be assumed without lack of generality that $\xi = +k_p$ occurs first, say at $t = t_{11}$ (Fig. 2.3). For $t \geq t_{11}$, and as long as only the p^{th} storey yields,

$$\ddot{u}_p = \xi - \frac{V_{op}}{\sum_{j=p}^N m_j} = \xi - k_p \quad (2.08)$$

$$\ddot{u}_i = 0 \quad (i \neq p)$$

These equations hold as long as*

$$V_i = \xi \sum_{j=i}^{p-1} m_j + (\xi - \ddot{u}_p) \sum_{j=p}^N m_j < V_{oi} \quad (i < p) \quad (2.09)$$

Let

$$\frac{V_{oq} - V_{op}}{\sum_{j=q}^{p-1} m_j} = \min \left[\frac{V_{oi} - V_{op}}{\sum_{j=i}^{p-1} m_j} \right] = k_q \quad (i = 1, \dots, p-1) \quad (2.10)$$

and note that, as it can be easily proved, Eq. (2.07) implies

$$k_q > k_p \quad (2.11)$$

* Since it has been already demonstrated that yielding cannot "move upwards," it is only necessary to consider storeys below the p^{th} .

If $\xi(t)$ remains always smaller than k_q , no other storey but the p^{th} is ever yielded, and the response of the frame is again a one-degree-of freedom motion, for which the results of Section 1 apply.

Suppose now that a certain time, say t_{15} (Fig. 2.3),

$$\xi(t_{15}) = k_q \quad (2.12)$$

Then, Eqs. (2.08) hold only in the interval

$$t_{11} \leq t \leq t_{15} \quad (2.12)$$

while for $t > t_{15}$ it can be easily derived

$$\begin{aligned} \ddot{u}_p &= k_q - k_p \\ \ddot{u}_q &= \xi - k_q \\ \ddot{u}_i &= 0 \quad (i \neq p, q) \end{aligned} \quad (2.13)$$

i.e. two storeys are yielding: in other words, two "simple mechanisms" are active at the same time; the acceleration of the first mechanism remains constant, while that of the second is graphically immediate (dot-shaded in Fig. 2.3).

It would be quite simple to derive further values of the ground accelerations which activate further mechanisms, and to write the relevant expressions for the storey accelerations, analogous to (2.13).

Suppose instead that $\xi(t)$ satisfies the periodicity conditions (1.06) and that its maximum value ξ_m is such that only the two already considered mechanisms can be activated.

The motion beyond $t > t_{15}$ is governed by Eqs. (2.13) as long as

$$\dot{u}_q = \int_{t_{15}}^t \ddot{u}_q dt \geq 0 \quad (2.14)$$

i.e. up to the time t_{16} , defined by

$$\int_{t_{15}}^{t_{16}} (\xi - k_q) dt = 0 \quad (2.14')$$

or graphically, in the example of Fig. 2.3,

$$A_2 = A_3 + A_4 \quad (2.15)$$

At $t = t_{16}$, the velocity of the first mechanism is

$$\dot{u}_p(t_{16}) = \int_{t_{11}}^{t_{16}} \ddot{u}_p dt = A_1 + A_3 ; \quad (2.16)$$

Eqs. (2.08) are again valid beyond t_{16} , up to the instant t_{12} defined by

$$\dot{u}_p(t_{12}) = \int_{t_{11}}^{t_{12}} \ddot{u}_p dt = \int_{t_{11}}^{t_{15}} (\xi - k_p) dt + \int_{t_{15}}^{t_{16}} (k_q - k_p) dt + \int_{t_{16}}^{t_{12}} (\xi - k_p) dt = 0 \quad (2.17)$$

or, graphically, by

$$A_1 + A_3 = A_5 \quad (2.18)$$

But Eqs. (2.15) and (2.18) imply

$$A_1 + A_2 = A_4 + A_5 \quad (2.19)$$

i.e. the time t_{12} , at which the velocity of the first mechanism \dot{u}_p becomes zero, can be determined ignoring the existence of the second mechanism. (This result holds for any value of $\xi(t_{12})$.)

The further motion beyond t_{12} can be easily constructed by similar arguments. Analogous to Section 1, if

$$\xi(t_{12}) \geq -k_p, \quad (2.20)$$

for the assumed periodic-symmetric $\xi(t)$, the negative velocity pulse begins at

$$t_{13} = t_1 + \frac{T}{2} \geq t_{12} \quad (2.20')$$

and a periodic motion is thus started, with the same period as the forcing function $\xi(t)$, and comprising intervals in which none, one and two mechanisms are active.

If Eq. (2.20) is not satisfied, the same arguments developed in Section 1, prove that the response tends to a steady state periodic motion whose acceleration diagrams can be most easily determined taking advantage of the property (2.19), as shown in Fig. 2.4.

Namely, the instants

$$t_{11}^*, t_{12}^* = t_{11}^* + \frac{T}{2}, t_{21}^* = t_{11}^* + T, \dots \quad (2.21)$$

at which $\dot{u}_p^s = 0$, are first determined by the condition

$$A_1^* + A_2^* = A_4^* + A_5^* = A_6^* + A_7^* = A_9^* + A_{10}^* = \dots \quad (2.22)$$

The second mechanism, in each cycle of the steady state response, is activated at $t = t_{n5}^*$ and $t = t_{n7}^*$, which coincide with t_{n1}^* and t_{n2}^* if

$$\xi(t_{n1}^*) = -\xi(t_{n2}^*) \geq k_q \quad (2.23)$$

as in the example in Fig. 2.4. This second mechanism stops at the instants

$$t_{n6}^* \quad \text{and} \quad t_{n8}^* = t_{n6}^* + \frac{T}{2} \quad (2.24)$$

given by

$$A_2^* = A_3^* + A_4^* = A_7^* = A_8^* + A_9^* \quad (2.24')$$

and certainly distinct from t_{n2}^* and $t_{(n+1)1}^*$.

The derivation of the response of each relevant mechanism, discussed above, leads for each mechanism to the same conclusions reached in Section 1.

Finally, note also that the symmetry of the frame behavior with respect to the sign of the load implies only that positive and negative limit shear forces (2.01) are equal. This condition is less stringent than the general one; for instance, it is satisfied if the moment-axial load yield profiles of the columns are symmetric with respect to the axial load axis but not with respect to the origin (as is the case for reinforced concrete columns); and it may be satisfied even if the individual columns have different positive and negative limit moments, provided they are suitably arranged.

By the same token, we can add constant loads on the structure (e.g. vertical loads on the columns), and thus change only the numerical value of M_{oj} and, consequently, of V_{oi} (2.01), provided the symmetry of the latter with respect to the variable (horizontal) loads is not affected. (This conclusion does not take into account the possible instabilizing effect of the vertical loads, which will be considered in Section 4).

3. THREE-DIMENSIONAL "SHEAR FRAMES" SUBJECTED TO HORIZONTAL LOADS

As it has been pointed out in the previous section, in most actual instances of rigid-plastic shear frames only the first storey yields under horizontal loads. For the purpose of the present study, the frame thus reduces to a single rigid mass

$$m = \sum_{i=1}^N m_i \quad (3.01)$$

supported by a number of rigid-plastic columns. The inertia forces, being applied at a finite height over the top of the columns, cause differential axial loads in the columns: if the effects of these loads are neglected (as they have been implicitly in Section 2), the rigid mass can be further reduced to a platform of vanishing depth (Fig. 3.1).

This Section 3 is concerned with the behavior of a frame thus simplified, when the columns are not all coplanar. The static collapse under a horizontal force P is discussed first in Subsection 3.1, then Subsection 3.2 deals with the dynamic response to a time-dependent force P or a horizontal ground acceleration \ddot{u}_g . Note that the loads P and \ddot{u}_g have been underlined (as all other relevant quantities in this section will also be), in order to stress their two-component vectorial character.

The plastic dynamic behavior of three-dimensional frames of a similar type has never been examined before, to the writer's knowledge, although it seems to be a realistic model of buildings in which architectural or functional reasons prevent bracing in any vertical plane, at least at the first (ground) storey level. Therefore, the problem studied herein, besides being an interesting example of a multi-mechanism response of a type not yet considered, is also of direct technical relevance, and well worth some further attention. Although only

preliminary results are presented, there seems to be no conceptual difficulty in their application and generalization. In fact, at least under some limitative conditions, the rigid-plastic hypothesis already allows to derive some rather general qualitative indications and to define some properties essential for further analyses of a more quantitative nature.

3.1 Static Collapse

The static collapse of the frame in Fig. 3.1, which has been the object of recent works by Harrison [1968] and Wittrick [1968], can be described as an elementary rotation $d\phi$ of the rigid platform about a vertical axis c . In the following, it will be assumed (as already done by both Harrison and Wittrick) that the torsional strength of the columns is negligible in comparison with their bending strength in any plane. It is then very easy to find the collapse value P_0 and the line of action, f , of the force P associated to each axis of rotation c (although sometimes P_0 is not defined uniquely for a given c , as it will be seen).

Let C and B_j (Fig. 3.2a) be the traces on a horizontal plane of the axis of rotation c and of the axis of the j^{th} column respectively: let further ϕ_{Mj} be the yield profile for biaxial bending of the same column*. The axes of the plastic hinges developing in the top and bottom cross-sections of the column are parallel to CB_j ; the corresponding yield moment vectors M_{oj} are obtained from the normality rule (Fig. 3.2a); the shear force in the yielding column is orthogonal to the moment vectors and of magnitude

$$V_{oj} = 2 \frac{M_{oj}}{h} \quad (3.02)$$

for a column of length h built-in at both ends.

* Yield profiles of structurally significant sections, including the effect of axial load, have been recently presented by S. Santathadaporn and W. F. Chen [1968].

Alternatively (Fig. 3.2b), the moment yield profile can be rotated by 90° and divided by $h/2$ to obtain the shear yield profile ϕ_{vj} of the j^{th} column.* The normality rule can then be applied directly to obtain the shear yield force V_{oj} from the elementary displacement

$$du_j = d\rho \times CB_j \quad (3.03)$$

This alternate procedure is slightly more general, because it includes the cases in which the shear yield profile is obtained less immediately from the moment profile (e.g., when the bottom section of the column is pinned in one direction only, or when the top and bottom sections of the column are different from each other).

In the more general situation, the vectorial sum of the V_{oj} gives uniquely the collapse force associated with C

$$P_o = \sum_j V_{oj} \quad (3.04)$$

Indeterminacies arise whenever a shear yield profile has a straight segment normal to du_j , and in the particular case of C coinciding with one of the B_j , say with B_n .

In the last case, the n^{th} term in the sum (3.04) is only required not to violate ϕ_{Vn} and is otherwise arbitrary. Wittrick [1968] has shown that this situation arises when the foot of the perpendicular from B_n to f falls within a plane domain, called safe zone of the n^{th} column and given by a very simple geometrical transformation of ϕ_{Vn} .

* The shear yield profile thus defined is not connected with a "shear failure" of the column, but with the "shear force" which, at the collapse limit, equilibrates the moments in the plastic hinges formed at the ends of the column.

On the other hand, if C is at infinity, i.e. if the collapse motion of the platform is a translation, all \underline{du}_j are equal, say to \underline{du} : however, the associated \underline{V}_{oj} are in general different and not parallel to each other. By varying the direction of the translation \underline{du} , the value and the line of action of \underline{P}_o (3.04) are changed. If the \underline{P}_o associated with all possible translations are drawn with origin in the same point, their end points describe a closed convex curve, symmetric with respect to the origin, that can be called total shear yield profile (or more simply yield profile) of the frame Φ_p : the normality rule between Φ_p and \underline{du} holds.

On the contrary, it does not appear possible to give an evident geometrical condition or property satisfied by the lines of action f of \underline{P}_o corresponding to translational collapse. This is shown by the comparatively very simple example in Fig. 3.3, pertaining to a platform supported on three I-section columns B_1 , B_2 , B_3 whose yield profiles are Φ_{V1} , Φ_{V2} , Φ_{V3} respectively: each translation vector \underline{du}_i and the corresponding line f_i are labeled by the same suffix.

Fortunately, in a number of instances of practical interest a point C_p exists such that, when f passes through C_p with any inclination, the collapse motion is a translation. Such a point C_p can be well defined as the plastic shear center C_p of the frame. (Note however that C_p is defined by a purely sufficient condition, which does not exclude that a \underline{P}_o with line f not through C_p may also cause translational collapse.) Examples of C_p are as follows:

- a) if the plan of the columns has two axes of symmetry, C_p coincides with their intersection;
- b) if the shear yield profiles of the single columns Φ_{Vj} are all similar to each other, say in ratios s_j , and similarly

oriented, any \underline{du} is (or can be) associated with yield forces \underline{V}_{oj} parallel to each other and in ratios $s_j : C_p$ is therefore the centroid of masses proportional to s_j concentrated in B_j . (This example is always verified when the ϕ_{vj} are circles.)

c) if the ϕ_{vj} are rectangles defined by

$$|V_{xj}| \leq V_{oxj} \quad (3.05)$$

$$|V_{yj}| \leq V_{oyj}$$

C_p is given by the intersection of the resultants of V_{oxj} and V_{oyj} .

3.2) Dynamic Behavior

The behavior of the frame in Fig. 3.1, subjected to a time-dependent force applied in the centroid C_G

$$\underline{P} = m \underline{\xi}(t) \quad (3.06a)$$

or to a horizontal ground acceleration

$$\ddot{\underline{u}}_g = -\underline{\xi}(t) \quad (3.06b)$$

will now be examined. For the sake of simplicity, in the following discussion it will be assumed (i) that the magnitude and the sign, but not the direction of $\underline{\xi}$, vary in time, and (ii) that the plastic shear center C_p exists and coincides with the centroid of the platform C_G (as it does in example a) at the end of Section 3.1). The frame is thus loaded at any instant by a total resultant force applied in the plastic shear center

$$\underline{F} = m(\underline{\xi} - \ddot{\underline{u}}) \quad (3.07)$$

where \ddot{u} is the acceleration of the platform relative to the base plane (Fig. 3.4a). The motion is a translation whose instantaneous velocity \dot{u} satisfies the normality rule with respect to the yield profile of the frame ϕ_p . In analogy with Sections 1 and 2, it is convenient to divide the yield profile by m ; the profile thus obtained will be denoted by ϕ and its equation symbolically indicated by

$$\phi(k_x, k_y) = 0 \quad (3.08)$$

(Fig. 3.4b). Then, letting

$$\begin{aligned} \underline{OX} &= \underline{\xi} = \underline{\xi}(\xi_x, \xi_y) \\ \underline{LX} &= \underline{u} = \underline{u}(\ddot{u}_x, \ddot{u}_y), \end{aligned} \quad (3.09)$$

the conditions governing the motion, analogous to Eqs. (1.02), can be stated as follows:

- a) when $\dot{u} \neq 0$ and/or $\ddot{u} \neq 0$, the total loading point L is on the yield curve ϕ , and \dot{u} is directed as the outward normal to ϕ in L (Fig. 3.4b);

$$\phi(k_x, k_y) = \phi(\xi_x - \ddot{u}_x, \xi_y - \ddot{u}_y) = 0 \quad (3.10)$$

$$\frac{\left(\frac{\partial \phi}{\partial k_x}\right)\bigg|_L}{\left(\frac{\partial \phi}{\partial k_y}\right)\bigg|_L} = \frac{\dot{u}_x}{\dot{u}_y} = \frac{\dot{u}_{x0} + \int_{t_0}^t (\xi_x - k_x) dt}{\dot{u}_{y0} + \int_{t_0}^t (\xi_y - k_y) dt}$$

where t_0 is the initial instant of motion and \dot{u}_{x0} , \dot{u}_{y0} the components of a possible initial velocity \dot{u}_0 . If L coincides with a pointed vertex of ϕ , the usual well known generalizations of Eqs. (3.10) apply.

b) when $\dot{u} = 0$ and X is not external to Φ ,

$$\phi(\xi_x, \xi_y) \leq 0 \quad (3.11)$$

$$\ddot{u} = 0 \quad (X \equiv L)$$

All the information on the motion might be obtained from two plots, analogous to those used in Sections 1 and 2, namely

$$\begin{aligned} \text{a) } \ddot{u}_x &= \xi_x - k_x \text{ vs. } t \\ \text{b) } \ddot{u}_y &= \xi_y - k_y \text{ vs. } t \end{aligned} \quad (3.12)$$

where $\xi_x(t)$ and $\xi_y(t)$ are given and proportional to each other by assumption, $k_x(t)$ and $k_y(t)$ are such that either (3.10) or (3.11) are verified. However, the variation of k_x and k_y with t is not known a priori and the diagrams (3.12) can be in general obtained only by some form of successive approximation procedure.

For the following discussion, it is useful to define a principal direction of the yield profile as the direction of a straight line η_i through the origin, orthogonal to the yield profile in the points of intersection I_i and I_i' (e.g. η_1, η_2 in Fig. 3.5a). If I_i and I_i' are vertices of the yield profile, the definition is generalized by requiring η to be comprised in the fan of normals to the yield profile in I_i or I_i' (e.g. η_2, η_3, η_5 in Fig. 3.5b). Consider now a straight line $\bar{\eta}_i$ slightly rotated around 0 with respect to η_i : the tangential component θ_i of an outward vector directed along $\bar{\eta}_i$ can either point towards the original position η_i , or away from it (e.g., respectively θ_1 and θ_2 in Fig. 3.5a). If the first condition is verified on both sides of η_i , it will be said that the principal direction η_i is stable; viceversa, η_i is said to be unstable if the second condition is verified, at

least on one side. The physical reason for the use of these terms will soon become apparent: examples of unstable principal directions are η_2 in Fig. 3.5a, η_2 , η_3 , η_5 in Fig. 3.5b. Because of the symmetry of Φ with respect to the origin, at least two principal directions always exist, of which one is stable and the other unstable.

If the loading vector ξ is directed along a principal direction η , also the acceleration \ddot{u} and the velocity \dot{u} are at all times parallel to η ; the total loading point L lies in the segment of η not external to the yield profile. In other words, the response involves only one degree of freedom, the two diagrams (3.12) are proportional to each other, and the whole discussion in Section 1 is fully applicable.*

On the contrary, if ξ is not parallel to a principal direction, the acceleration \ddot{u} and the velocity \dot{u} change direction with time, and the motion is a two-degree-of-freedom translation. If the vectors \dot{u} at successive instants are reported from a common origin O_v ,

$$\underline{O_v U} = \dot{u} = \dot{u}_0 + \int_{t_0}^t \ddot{u} dt \quad (3.13)$$

(where a vector integral appears), their end point U describes a trajectory v , whose tangent in any instant is parallel to the corresponding \ddot{u} .

As a first example, consider the response to an impulse, corresponding to an initial velocity \dot{u}_0 applied at time $t = 0$ (Fig. 3.6a).** For any $t > 0$,

* If ξ is parallel to η at every storey, the developments in Section 2 are valid for a multi-storey three dimensional shear frame as well. Otherwise, the latter structure must be analyzed by generalizations of the procedures outlined in this section.

** An impulsive loading problem of a similar type, applied to a lumped-mass cantilever beam, has been the subject of a very recent paper by Frick and Martin [1968].

$$\xi = 0, \quad \text{i.e. } X \equiv 0 \quad (3.14a)$$

and, in the interval $0 < t < t_f$

$$\ddot{u} = L_0 \quad (3.14b)$$

The initial position L_0 of L is determined by the requirement of normality between ϕ and \dot{u}_0 and gives the initial tangent to the v -trajectory (Fig. 3.5b). From the qualitative construction of v reported in Fig. 3.6b, it is evident that the final tangent to v is parallel to a stable principal direction. In other words, after the impulse, the total loading point L moves along the yield curve in the direction determined by the relevant tangential component of \ddot{u}_0 ; when the motion stops, L has reached but not passed the first stable point of intersection I_1 .

It is thus evident that, if the direction of the impulse is slightly rotated with respect to a stable principal direction, the response varies only slightly; while even a very little deviation of the load vector from an unstable principal direction causes a large difference at least in some aspects of the response (like the movement of L along ϕ). In other words, the one-degree-of-freedom response is fully reliable only when the loading vector is directed along a stable principal direction. This property, which appears to hold for any loading history, justifies the terms stable and unstable; however, it is not yet clear in general terms how the variation in the movement of L affects the structural response.*

The motion of L along ϕ need not be regular or continuous. Take for instance the most simple case of impulsive loading illustrated in Fig. 3.7. Initially, L remains in L_0 for a finite time interval, while

* Note also that most of the considerations just developed with regard to the load $\xi \cdot \ddot{u}$, yield profile and velocity \dot{u} of this particular structural model, apply also to the stress vector, yield surface and strain vector in each point of a rigid-perfectly plastic three-dimensional continuum.

$$\ddot{u}(\ddot{u}_y, \ddot{u}_x) = \underline{L_0} 0 (-k_1, -k_2) = \text{const} \quad (3.15)$$

$$(0 < t < t_1)$$

At $t = t_1$, the velocity vector \dot{u} becomes parallel to x ; L jumps to L_1 , then stays there while both \dot{u} and \ddot{u} remain horizontal,

$$\ddot{u}(\ddot{u}_y, \ddot{u}_x) = \underline{L_1} 0 (0, -k_2) = \text{const} \quad (3.15')$$

$$(t_1 < t < t_f)$$

The motion finally stops at $t = t_f$. The v -trajectory is constituted by two straight segments (Fig. 3.7b); the velocity-time diagrams are immediate (Fig. 3.7c, d).

As a further example, consider a frame whose strength in one particular direction, say x , is much larger than both the strength in the orthogonal direction y , and the maximum x -component of external load, ξ_{xm} . In this case, the yield profile can be approximated by two parallel straight lines (Fig. 3.8a)

$$k_y = \pm k_1 \quad (3.16)$$

and, although both X and L vary with time, \dot{u} and \ddot{u} are parallel to y for any loading history, i.e.

$$\ddot{u}_x = \xi_x - k_x \equiv 0; \quad \dot{u}_x \equiv 0 \quad (3.17)$$

The motion can be studied as in Section 1 for the non-vanishing component (Fig. 3.8b)

$$\ddot{u}_y = \xi_y - k_y = \xi_y \mp k_1 \quad (3.17')$$

Finally, if the yield profile of the frame is a rectangle with sides parallel to x and y , as in example a) at end of Section 3.2, the two component diagrams (3.12) can be studied independently of each other following the procedures outlined in Section 1. In particular,

$$k_y = \begin{cases} +k_1 & \text{when } \dot{u}_y > 0 \\ -k_1 & \text{when } \dot{u}_y < 0 \end{cases} \quad (3.18a)$$

$$k_x = \begin{cases} +k_2 & \text{when } \dot{u}_x > 0 \\ -k_2 & \text{when } \dot{u}_x < 0 \end{cases} \quad (3.18b)$$

Both x and y are stable principal direction of the yield profile, its diagonals are unstable principal directions.

If the maximum x-component of the load, ξ_{xm} , (Fig. 3.9) is not larger than k_2 , the response is the same one-degree-of-freedom just described with reference to Fig. 3.8.

On the contrary, Figs. 3.9 and 3.10 describe qualitatively the steady-state velocity under a periodic-symmetric loading history, such that both components fall in Case II defined in Section 1.2. (Note that, by an arbitrary choice of scale, the $\xi_x(t)$ and $\xi_y(t)$ diagrams have been drawn equal.) Inspection of the velocity diagrams shows that \dot{u} never vanishes: the normality rule requires the total loading point L to jump from one vertex to the other around the yield profile (from L_1 to L_2 to L_3 to L_4 to L_1 , etc.), remaining in each vertex for a finite time interval, indicated at the bottom of Fig. 3.10. The curve v , already defined, is shown in Fig. 3.9b: it is (in the steady-state motion) a closed curve, symmetric with respect to the origin O_v .

The motion of L around the yield profile is slightly more complicated if one of the component motions (or both) falls in Case I (Section 1.1), as in the example qualitatively illustrated in Figs. 3.11 and 3.12. Namely, L jumps from L_1 not directly to L_2 , but to an intermediate point L_{12} ; then it moves gradually towards L_2 in the interval (t_{x2}, t_{x3}) , while both \dot{u}_x and \ddot{u}_x remain zero. The same happens between L_3 and L_4 .

In all described examples (Figs. 3.7, 3.9, 3.11), the jumps of the total loading point L along the contour of the yield profile Φ (i.e. discontinuities in the acceleration vector $\ddot{u} = \underline{LX}$) are connected with the existence of straight-line segments in Φ , and the ensuing discontinuities in the points associated with a continuously varying velocity vector.

Results essentially similar to those derived in the above discussion can be also obtained with more general, curvilinear yield profiles, although the actual computation of the whole motion would probably require a rather complicated successive approximation procedure. It seems however possible to state that the steady state response of the three-dimensional frame under consideration, when subjected to a horizontal periodic-symmetric load, is a periodic translation with the same period as the loading, of which three subcases can be distinguished:

- a) if the load is directed along a principal direction of the yield profile, the response is a one-degree-of-freedom translation, parallel to the same direction;
- b) if the direction of the load is sufficiently close to a stable principal direction, the total loading point L moves in two distinct intervals of the contour of Φ , and the velocity vanishes twice during each cycle; the v-curve has an 8-shape;

- c) if neither a) nor b) are verified, the velocity never vanishes; L moves around the yield profile, possibly with some jumps. The signs of the rotations of the total loading point L around the yield profile ϕ and of the velocity point U around the v -trajectory appear to be both determined by the sign of the angle between the direction of ξ and the outward normals to ϕ in the points of intersections: e.g., it is clockwise when the loading vector is directed as ξ_1 in Fig. 3.13, anticlockwise when the load is directed as ξ_2 .

Note that there is no continuity between the motions of L associated with loads directed along an unstable principal direction and along a slightly rotated direction.

In conclusion, the considerations developed in this section, although still very far from practical applicability, have yielded some general indications on a two-degree-of-freedom response to dynamic load, in which the change of mechanism is due to the interaction between two generalized stress components and not to the formation or spreading of plastic zones. The distinction between stable and unstable principal directions can be of great interest in actual problems.

It appears that successive approximation procedure could be set up without excessive difficulties, for the computation of the motion of the specific type of frames so far examined, in which it will be recalled that $C_p \equiv C_G$ by assumption.

If C_p does not exist or does not coincide with C_G , the response is much more complicated, in that it involves a third degree of freedom, namely

a rotation about a vertical axis. Although this problem has not been investigated at all, no particular obstacle seems likely to arise in the extension of the arguments developed above, with the obvious exception of greatly increased computational difficulties.

4. EFFECTS OF GRAVITY ON THE DYNAMIC BEHAVIOR OF SHEAR FRAMES

In a frame such as those examined in Section 2, at each storey level the columns are subjected to compressive axial loads due to the weight of the upper floors, and the limit moments M_{oj} are consequently modified. As already pointed out at the end of Section 2, this effect can be easily accounted for in the dynamic analysis developed there, just by substituting the modified limit moments in the expressions of the frame shear strengths (2.01) at each storey level (provided, of course, that the shear strengths are not further significantly modified by the additional column axial loads due to the horizontal loads).

The present section will rather be concerned with the combined instabilizing effect of gravity loads W and horizontal displacements u in a plane shear frame, whose dynamic response involves yielding of the lowest storey only and which therefore can be diagrammatically represented as in Fig. 4.1. (The number of columns, as pointed out already in Section 2, is irrelevant). The following discussion could easily be extended to cover analogous instability effects in the single-mechanism dynamic responses of other structures.

With reference to Fig. 4.1 as compared to Fig. 1.1, Eqs. (1.02) are modified into

$$\begin{aligned}\ddot{u} &= \xi - k + Gu & \text{when } \dot{u} > 0 \\ \ddot{u} &= \xi + k + Gu & \text{when } \dot{u} < 0 \\ \ddot{u} &= 0 & \text{when } \dot{u} = 0 \text{ and } -(k + Gu) \leq \xi \leq (k - Gu)\end{aligned}\tag{4.01}$$

where

$$\xi = \frac{P}{m} \quad \text{or} \quad \xi = -\ddot{u}_g\tag{4.02}$$

measures the horizontally applied load, and

$$k = \frac{V_o}{m} = \frac{\Sigma M_o}{mh} \quad (4.03)$$

$$G = \frac{\Sigma W}{mh} = \frac{g}{h} ;$$

in turn, g is the acceleration of gravity.* Other expressions for k and G would be appropriate for other structural types.

In the ξ vs. t diagrams, already several times used in the present report, the effect of gravity loads is a vertical translation $G u$ of the strength interval ($+k$, $-k$), downwards when u is positive, upwards when u is negative (Fig. 4.2).

4.1 Impulsive Load

Consider first the response to an impulsive load, i.e. to an initial positive velocity \dot{u}_o . Eqs. (4.01) give

$$\ddot{u} - Gu = -k \quad (4.03)$$

for any $t > 0$, as long as $\dot{u} \geq 0$. The solution of Eq. (4.03), with the initial conditions

$$u(0) = 0 ; \quad \dot{u}(0) = \dot{u}_o > 0 \quad (4.04)$$

yields

$$\begin{aligned} u &= \frac{k}{G} (1 - \cosh \sqrt{G}t) + \frac{\dot{u}_o}{\sqrt{G}} \sinh \sqrt{G}t \\ \dot{u} &= \dot{u}_o \cosh \sqrt{G}t - \frac{k}{\sqrt{G}} \sinh \sqrt{G}t \\ \ddot{u} &= -k \cosh \sqrt{G}t + \dot{u}_o \sqrt{G} \sinh \sqrt{G}t \end{aligned} \quad (4.05)$$

* In a building frame, h is of order 10-15 ft; hence

$$G \approx 2-3 \text{ sec}^{-2} \text{ approx.}$$

which easily reduce to (1.03) when $G \rightarrow 0$.

The response velocity \dot{u} vanishes at a time $t = t_f$, given by

$$\tanh \sqrt{G} t_f = \frac{\dot{u}_o \sqrt{G}}{k} \quad (4.06)$$

Since

$$0 \leq \tanh x < 1 \quad \text{when} \quad 0 \leq x < \infty$$

Eq. (4.06) yields a real positive total response time t_f only if

$$\frac{\dot{u}_o \sqrt{G}}{k} < 1 \quad (4.08)$$

If (4.08) is not verified, the velocity successive to the impulse never vanishes, i.e. the frame never comes to a stop and deforms up to complete collapse.*

This result can be presented in several alternative ways. For example, introducing (4.03), disequality (4.08) becomes

$$(m \dot{u}_o)^2 h \frac{g}{(\sum M_o)^2} < 1 \quad (4.09)$$

and yields a limit relationship between the sum of the column flexural strengths (possibly, modified by the axial loads), the storey height h , and the impulse momentum $m \dot{u}_o$ that a rigid-plastic shear frame can absorb without complete collapse.

The variation of velocity with time for several values of $\frac{\dot{u}_o \sqrt{G}}{h}$, and the relationship between $\frac{\dot{u}_o \sqrt{G}}{h}$ and the total response time, given respectively by

* Remember, however, that the previous equations remain quantitatively valid only as long as the displacement u is small in comparison with h .

the second Eq. (4.05) and by Eq. (4.06), are plotted with solid lines in Fig. 4.3; the dotted lines represent the relationships valid when the instabilizing effect is neglected. The difference of behavior when (4.08) holds and when it does not is very evident: in the latter case, the velocity decreases at first, reaches a minimum and then increases monotonically up to the ruin of the frame.*

4.2 Periodic Load

The rest of the present section deals with the response given by Eqs. (4.01) when the load function $\xi = \xi(t)$ is periodic-symmetric, as already defined by Eqs. (1.06). Comparing Fig. 4.2 with the consideration developed in Section 1, it is immediate that the response $u(t)$, although involving successive plastic deformations of alternate signs, cannot be periodic: in fact, as soon as $u \neq 0$, an asymmetry of the effective strength tends to increase the residual displacements of a defined sign, which build up during the successive loading cycles, until the critical displacement

$$u_c = u(t_c) = \pm \frac{k}{G} \quad (4.10)$$

is reached, at which point the strength of the frame, with respect to horizontal loads of either positive or negative sign, becomes zero.**

The critical time (or time to collapse) t_c can be physically defined by the ability acquired by the gravity loads, to cause by themselves collapse of

* Similar results were obtained by Lee and Martin for a rigid-plastic column subjected to a particular type of transverse impulse [1966], but at the expense of rather cumbersome algebra that made the ultimate results much less immediately evident than the present ones.

** Strain-hardening with Bauschinger effect would also cause a translation of the strength interval $(-k, +k)$, but in a stabilizing direction: the response would tend to a periodic response, in which even the displacements are symmetric. Thus, if both strain-hardening and gravity loads are significant, their effects are opposite to each other, and either can prevail. [Augusti, 1969].

the frame. In other words, if a periodic loading $\xi(t)$ is applied for a finite number of cycles \bar{n} , the frame collapses (because of the constant axial loads) if, and only if,

$$\bar{n}T > t_c \quad (4.11)$$

or otherwise, if

$$\bar{n} > n_c \quad (4.11')$$

where the critical number of cycles n_c is defined by

$$n_c T \leq t_c < (n_c + 1)T \quad (4.12)$$

There is no conceptual difficulty in the numerical or analytical step-by-step integration of Eqs. (4.01) for any given loading program, and in the direct determination of the critical time t_c or critical cycle n_c , which will of course depend on the characteristics of the frame and on the shape of the loading function. Essentially this approach has been used in recent papers by Jennings and Husid [1968] (where an elasto-plastic frame under an earthquake load is examined, following earlier works by Housner [1959, 1960] who appears to have been the first to discuss the phenomenon of collapse of plastic structural frames because of gravity loads) and by Ballio [1968] (who found an analogous behavior for a one-degree-of-freedom elasto-plastic column model and a simple periodic loading). The numerical process would be greatly simplified in any case by the rigid-plastic assumption: the response could be determined, cycle by cycle, by a successive approximation procedure, as outlined below with reference to Fig. 4.4.

Suppose that the displacement u_{n-1} [hence, the effective strengths $(k - Gu_{n-1})$ and $(-k - Gu_{n-1})$] at the beginning of the n^{th} cycle are known. Assume, as a first approximation, a straight line r for the further variation of Gu .

and perform the integrations described in Section 1 from t_{n1} up to a tentative t_{n2} : introduce the diagram of u , thus obtained, in the acceleration diagram (Fig. 4.4a), and repeat the operations until the resulting t_{n2} and Δu_{n1} are stabilized. The same procedure is then used to obtain t_{n4} and Δu_{n2} .

It can be noted that, if

$$\xi_m < 2k \quad (4.13)$$

the negative-velocity phases disappear (i.e., $\Delta u_{n2} = 0$) before the critical displacement u_c is reached.

4.3 Direct Determination of the Critical Cycle n_c Under Periodic Loading

For any practical structure, n_c can be expected to be rather large: in fact, if a structure is at all intended to undergo periodic loading, it is certainly required to be able to withstand more than a few cycles. In this case the rigid-plastic assumption appears to become really convenient, in that it will allow the direct determination of bounds to n_c without following the whole response history, as outlined below. It is still an open question whether the critical times thus calculated are realistic, although rough, approximations of the critical time of the actual, elastic-plastic frame.

The case corresponding to Case I of Section 1.1 is discussed first.

It is self-evident from Fig. 4.4 that the net variation of u in each cycle

$$u_n - u_{n-1} = \Delta u_{n1} - \Delta u_{n2} \quad (4.14)$$

increases with n : hence

$$u_n > n(\Delta u_{11} - \Delta u_{12}) \quad (4.15)$$

where the displacement increments during the first loading cycle $(\Delta u_{11}, \Delta u_{12})$ can be obtained as in Fig. 4.4, with a zero initial displacement

$$u_{n-1} = u_0 = 0 \quad (4.16)$$

Eqs. (4.10) and (4.15) give an upper bound to n_c in the form

$$n_c < n_{c+} = \frac{k}{G(\Delta u_{11} - \Delta u_{12})} \quad (4.17)$$

To determine a lower (safe) bound to n_c , suppose that a displacement u_{m-1} can be chosen, such that performing the operations in Fig. 4.4,

$$u_{m-1} + \Delta u_{m1} \leq \frac{k}{G} \quad (4.18)$$

$$u_m + \Delta u_{(m+1)1} > \frac{k}{G}$$

In other words, if u_{m-1} were actually the displacement at the beginning of the m^{th} cycle, $m = n_c$. Then, by the same argument leading to (4.17),

$$n_c > n_{c-} = \frac{k}{G(\Delta u_{m1} - \Delta u_{m2})} \quad (4.19)$$

The bounds (4.17) and (4.19) are diagrammatically indicated in Fig. 4.5a.

A value for u_{m-1} can be obtained in the following way (Fig. 4.6a). Choose a time t_{m2} , draw a line r such that $A_{m1} = A_{m2}$, then perform the integrations in Fig. 4.4 starting from t_{m1} and the corresponding u_{m-1} , and repeat until

$$u(t_{m2}) = u_{m-1} + \Delta u_{m1} = \frac{k}{G}. \quad (4.20)$$

If (4.13) holds,

$$-(k + Gu) = -2k < \xi \quad \text{at} \quad t = t_{m2} \quad (4.21)$$

and (4.18) are certainly verified. But note that if n_c is large as assumed, the inclination of r must be very small, and

$$t_{m2} = t_{m1} + T \quad (4.22)$$

therefore, it seems fair to assume that (4.21) holds also if (4.13) does not, with the only exception of loading programs of the type shown in Fig. 4.6b. Even in this very particular case, however, the procedure of Fig. 4.6a yields a very small Δu_{m2} , so that it can be assumed that (4.18) are again verified.

Consider now the case in which, if the effect of the axial loads were neglected, the conditions of Section 1.2 (or the so-called Case II) would be realized. Comparing Eqs. (4.15) and (1.28), it can be noted that the two opposite effects interact; however, in the long range, the instabilizing effect does prevail.

If the final residual displacement (neglecting axial loads) u_R is much smaller than the critical displacement u_c , it could be (unsafely) neglected altogether. In this case, Δu_{11} and Δu_{12} to be introduced in (4.17) must be computed starting from $u_0 = 0$ and t_{11}^* determined as in Fig. 1.4.

Conversely, if u_R can be at least approximately evaluated, it is safe to consider it acting from the very beginning of the loading: then, instead of n_c , a smaller number n_c^* is defined (Fig. 4.5b) and bounded between

$$n_{c+}^* = \frac{\frac{k}{G} - u_R}{\Delta u_{11}^* - \Delta u_{12}^*} \quad (4.23)$$

$$n_{c-}^* = \frac{\frac{k}{G} - u_R}{\Delta u_{m1} - \Delta u_{m2}}$$

Here, Δu_{11}^* and Δu_{12}^* must be determined with

$$u_{n-1} = u_0 = u_R \quad (4.24)$$

Even more simply, let $\Delta \bar{u}$ be the increment of displacement during a loading cycle calculated in the assumption that the (effective) shear strength of the frame is constantly nil (Fig. 4.7). $\Delta \bar{u}$ is an upper bound to the displacement of the frame in each cycle for both Cases I and II, so that a safe value of n_{c-} is given very quickly by

$$n_{c-} = \frac{k}{G \Delta \bar{u}} \quad (4.25)$$

Noting that

$$\Delta \bar{u} = \int_{t_{n1}}^{t_{(n+1)1}} dt \int_{t_{n1}}^t \ddot{u} dt = - \int_{t_{n1}}^{t_{(n+1)1}} (t - t_{n1}) \ddot{u} dt \quad (4.26)$$

is the first moment with respect to $t = t_{n1}$ of the two equal areas A_{01} and A_{02} in Fig. 4.7a (each taken with its sign) and that, because of (1.06), the centroids of A_{01} and A_{02} are $T/2$ apart, it is immediate that

$$\Delta \bar{u} = A_{01} \frac{T}{2} = \xi_a \frac{T^2}{4} \quad (4.27)$$

where ξ_a is the average absolute value of $\xi(t)$. In other words, the increment of displacement in a frame of zero strength during a cycle of periodic-symmetric loading, does not depend on the shape of the loading function, but only on its average value and the square of its period.

Introduction of (4.27) and (4.03) into (4.25) yields

$$n_{c-} = 4 \frac{kh}{g \xi_a T^2} = 4 \frac{\Sigma M_o}{\xi_a T^2 \Sigma W} \quad (4.28)$$

Although Eq. (4.28) can only be expected to give a very rough lower limit on n_c , it may be used to evaluate the qualitative effect of some parameters.

Of course, the motion of a rigid-plastic frame is excited only if the maximum value of the load, ξ_m , is larger than the frame strength k . In other words

$$n_c = \infty \quad \text{if} \quad \frac{\xi_m}{k} \leq 1 \quad (4.29)$$

Thus, any curve or formula for n_c has a lower cut-off, that can be written in the form

$$\frac{\xi_a}{k} = \frac{\xi_a}{\xi_m} \quad (4.30)$$

The ratio ξ_a/ξ_m is comprised between 0.5 and 1 for any "reasonable" loading function $\xi(t)$. Eqs. (4.28) and (4.30) are plotted in Fig. 4.8.

Finally, it is worth noting for comparison that, after lengthy numerical calculations of the responses of an elastic-plastic frame subject to random loading functions and statistical analyses of the results, Jennings and Husid concluded, in their already quoted paper [1968], that the average time to collapse was proportional to the storey height and to the square of the ratio between the strength of the frame and the average intensity of the ground acceleration; they did not investigate the effect of the frequency of the load. Introducing the present symbols and denoting by C an appropriate constant, Jennings and Husid's results can be represented by

$$(n_c T)_{\text{avg}} = Ch \left(\frac{k}{\xi_a} \right)^2 \quad (4.31)$$

The qualitative agreement between Eqs. (4.28-30) and Eq. (4.31) is remarkable: it has been shown [Augusti, 1969] that the quantitative agreement is also fairly good, and this would seem to support the opportunity for further researches of the type set forth in the present report.

SUMMARY AND CONCLUSIONS

The present report has discussed several aspects and examples of behavior of rigid-plastic structures subjected to dynamic loading.

In particular, in Section 1 it has been shown that the response of strength-symmetric structures to periodic-symmetric loading (in absence of the instabilizing effect examined in Section 4) is, or rapidly tends to, a periodic motion. In other words, the structure shakes down to a rigid-plastic vibration of limited amplitude and the same period as the external agency. The total accumulated plastic work (high strain fatigue) becomes the key factor of design.

Whenever the response mechanism is unique (as it is shown to be usually the case for plane shear frames subjected to horizontal loads), very simple semigraphical operations allow both to follow the response cycle by cycle and to determine directly the final (or steady-state) motion.

It has not been found possible, for a general loading program, to obtain a simple but rational approximation of the response, such as the mode approximation proposed by Martin and Symonds [1966] for impulsive loading problems and recently extended to single-pulse loads. In the particular case of plane shear frames, however, even the multi-mechanism response is governed by very simple relations.

On the contrary, the dynamic response of three-dimensional shear frames (studied in Section 3) is of rather cumbersome determination because two interacting degrees of freedom are involved, except in some very special cases. For example, the response to a periodic load is given by a cyclically variable, but in most cases never vanishing, horizontal velocity vector. It is, on the other hand, possible to define principal directions, such that if the load is parallel to one of them the response is one-degree-of-freedom, and distinguish them in stable and unstable.

Finally, in Section 4, the effect of constant gravity loads on the response of plane shear frames has been examined. Firstly, impulsively loaded frames have been considered, and a relationship has been established between the total column strength, the height of the ground storey, and the momentum that the frame can absorb without collapsing.

Then, it has been shown that, under periodic loads, plastic deformations of alternate sign develop, but the residual displacement increases with the loading cycles until, when a critical displacement is reached, the gravity loads become able to cause by themselves collapse of the frame. Formulae have been proposed to bound the number of cycles necessary to reach the critical displacements. Both high strain fatigue and collapse by gravity loads may be significant factors in the design of such frames.

Applications and numerical examples of the procedures outlined in this report are at present being developed and will be included in later papers.

The whole treatment presented here has been limited to the consideration of rigid-perfectly plastic behavior and has therefore the same limitations of all previous works which have been based on the same assumption. These limitations will not be discussed here, but it seems appropriate to note that two of them might be particularly relevant for the sort of problems treated in this report; namely,

- a) the yield stress (or yield profile) varies with the rate of deformation; this variation may not only cause quantitative differences (as in all dynamic plastic problems) but also alter the interaction between the different degrees of freedom;
- b) the elastic deformations under a periodic loading can be increased by resonance; their effect might be assimilated to

a substantial reduction of the (apparent) plastic strength.

While it must be stressed that the present study has no pretense to be conclusive, and that the above problems (and many others) can furnish a wealth of material for further investigations, it is also fair to remark that the simplifications inherent in the rigid-plastic assumption have allowed to obtain some fairly general indications regarding problems either never tackled before or solved only numerically.

ACKNOWLEDGMENTS

The Author's thanks are due to:

the American Commission for Cultural Exchanges with Italy, for the award of a Fulbright Travel Grant;

the Division of Engineering of Brown University, and in particular its Chairmen Professors P. F. Maeder and J. J. Loferski, for the financial support received and the facilities made available;

the Faculty of Engineering of Naples University, and in particular Professor Franciosi, Director of the "Istituto di Scienza delle Costruzioni," for granting the Author a leave of absence.

Finally, the Author wishes to acknowledge gratefully that this research would never have materialized without the frequent illuminating and stimulating discussions with Dr. J. B. Martin, Professor of Engineering at Brown University, who also read through drafts of this report.

NOTATION

A_1, A_2	areas (integrals of acceleration)
B_j	axis of j^{th} column (in horizontal plan)
c, C	axis and center of (elementary) rotation, Figs. 3.1-3.2
C_G, C_P	centroid and <u>plastic shear center</u> of frame in Fig. 3.1
F	total force (including inertia term)
f	line of action of force \underline{P}
G	parameter measuring the instabilizing effect of vertical loads in Eqs. (4.01)
g	acceleration of gravity
h	height of storey
I	intersection of η and yield profile
i	suffix for generic storey, loading cycle, etc.
J_i	number of columns at i^{th} storey of frame
k	strength parameter
L	<u>total loading point</u> or terminal point of vector $\underline{\xi} - \ddot{\underline{u}}$ (Fig. 3.4 ff.)
l	beam span (Fig. 2.1)
M	bending moment
M_0	limit (full yield) moment
m	mass
N	number of storeys in frame
n	number of loading cycles (also, suffix)
n_c	"critical" number of cycles
O	origin of reference axes or vectors

P	applied force
p, q	suffixes denoting particular storeys in multi-storey frame
T	period of time-dependent loads
t	time
t_c	"critical time" or "time to collapse" (Section 4.2)
t_f	total response time for impulsive loading
U	terminal point of vector \dot{u} (Fig. 3.6 ff.)
u	displacement
\dot{u}	velocity
\ddot{u}	acceleration
\ddot{u}_g	ground acceleration
u_R	residual displacement
$u^s, \dot{u}^s, \ddot{u}^s$	"steady state" displacement, velocity, acceleration
V_i	total shear force at i^{th} storey
V_{oi}	limit shear force (shear strength) of i^{th} storey
v	curve of points U
W	vertical loads on frame
X	<u>loading point</u> , or terminal point of vector ξ (Fig. 3.4 ff.)
x, y	coordinate axes (also, suffixes for x- and y-components of vectors)
Δu	displacement increment
n	<u>principal direction of yield profile</u> ϕ
$\xi = \xi(t)$	load parameter (function of time)
ξ_a	average absolute value of $\xi(t)$
ξ_m	maximum value of $\xi(t)$

ϕ yield profile
 $\phi = 0$ equation of yield profile

Notes:

- a) Underlined symbols indicate vectors (e.g. $\underline{\xi}$, $\dot{\underline{u}}$, etc.)
- b) Many other suffixes, asterisks, etc., have been often used to qualify several symbols.

REFERENCES

- Augusti, G., Discussion of the paper by Jennings and Husid quoted below; Journal of the Engineering Mechanics Div., A.S.C.E., 1969 (to be published).
- Augusti, G., Martin, J. B., and O'Keefe, J. D., "An Approximate Method of Analysis for Rigid-Plastic Pulse-Loaded Structures." Submitted for presentation at the 2nd Canadian Congress of Applied Mechanics; Waterloo, Ontario, May 1969.
- Ballio, G., "Elastic-Plastic Dynamic Behavior of a Beam-Column Model." Meccanica (Journal of the Italian Association of Theoretical and Applied Mechanics AIMETA), Milan, Vol. 3, No. 3, pp. 177-186, Sept. 1968.
- Frick, A. J., and Martin, J. B., "The Plastic Deformation of a Cantilever Subjected to Biaxial Bending by an Impulsive Load at its Tip," Report No. NSF-GK1013/15, Div. of Engineering, Brown Univ., Providence, R. I., June 1968
- Harrison, H. B., "The Ultimate Resistance to Horizontal Shear of a Simple Space Frame," Proceedings of the Institution of Civil Engineers, London, Vol. 39, No. 2, pp. 313-322, Feb. 1968.
- Housner, G. W., "Behavior of Structures During Earthquakes," Journal of the Engineering Mechanics Div., A.S.C.E., Vol. 85, No. EM4, pp. 109-129, Oct. 1959.
- Housner, G. W., "The Plastic Failure of Frames During Earthquakes," Proceedings of the Second World Conference on Earthquake Engineering, Tokyo and Kyoto, Vol. 2, pp. 997-1012, 1960.
- Jennings, P. C., and Husid, R., "Collapse of Yielding Structures During Earthquakes," Journal of the Engineering Mechanics Div., A.S.C.E., Vol. 94, No. EM5, pp. 1045-1065, Oct. 1968.
- Johnson, G. L., and Martin, J. B., "The Permanent Deformation of a Portal Frame Subjected to a Transverse Impulse," Report No. BU/DTMB/12, Div. of Engineering, Brown Univ., Providence, R. I., Aug. 1967.
- Kaliszky, S., "Approximate Solutions for Impulsively-Loaded Inelastic Structures and Continua." Presented orally at the 12th International Congress of Applied Mechanics, Stanford, Calif., Aug. 1968. (Full text to be published).
- Lee, L.S.S., and Martin, J. B., "The Behavior of a Rigid-Plastic Column Subjected to a Transverse Dynamic Disturbance," Report No. BU/DTMB/8, Div. of Engineering, Brown Univ., Providence, R. I., April 1966.

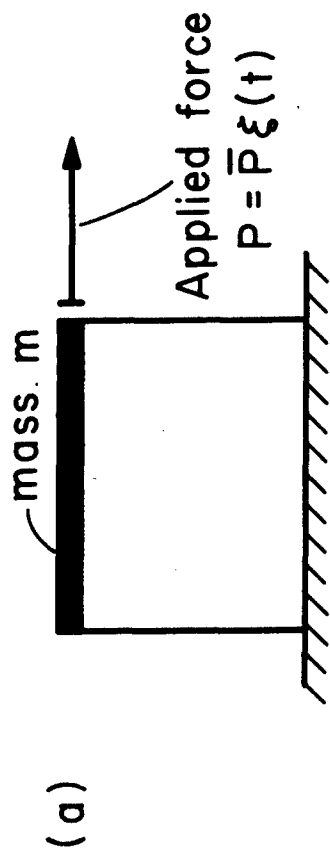
- Martin, J. B., "A Note on the Uniqueness of Solutions for Dynamically Loaded Rigid-Plastic and Rigid-Viscoplastic Continua," Journal of Applied Mechanics, A.S.M.E., Vol. 33, No. 1, pp. 207-209, March 1966.
- Martin, J. B., "Mode Approximations for Impulsively Loaded Structures in the Inelastic Range," to be published in the Proceedings of the International Conf. on Structure, Solid Mechs. and Engrg. Design in Civil Engineering Materials, Southampton, England, J. Wiley, 1969.
- Martin, J. B., and Lee, L.S.S., "Approximate Solutions for Impulsively Loaded Elastic-Plastic Beams," Journal of Applied Mechanics, A.S.M.E., Vol. 35, No. 4, pp. 803-809, Dec. 1968.
- Martin, J. B., and Symonds, P. S., "Mode Approximations for Impulsively-Loaded Rigid-Plastic Structures," Journal of the Engineering Mechanics Div., A.S.C.E., Vol. 92, No. EM5, Oct. 1966.
- Oien, M. A., and Martin, J. B., "Approximate Methods for Rigid-Plastic Structures Subjected to Dynamic Loading," Report No. BU/DTMB/7, Div. of Engineering, Providence, R. I., Aug. 1965.
- Santathadaporn, S., and Chen, W. F., "Interaction Curves for Sections Under Combined Biaxial Bending and Axial Force," Fritz Engineering Lab. Report No. 331.3, Dept. Civil Engrg., Lehigh Univ., Bethlehem, Penn., August 1968.
- Wittrick, W. H., "Sidesway Collapse Modes for Groups of Vertical Columns," Internat. Jour. Mechanical Sciences, Vol. 10, pp. 549-562, 1968.

LIST AND CAPTIONS OF FIGURES

- Figure 1.1 - Simple example of dynamically loaded structure.
- Figure 1.2 - Periodic-symmetric loading; Case I.
- Figure 1.3 - Periodic-symmetric loading; Case II.
- Figure 1.4 - Periodic-symmetric loading; Case II. Periodic solution.
- Figure 2.1 - Different multiple-mechanism behaviors of a dynamically-loaded simply-supported beam.
- Figure 2.2 - Shear frame.
- Figure 2.3 - Two-mechanism motion of rigid-plastic shear frame. (Load and acceleration diagrams.).
- Figure 2.4 - Two-mechanism motion of rigid-plastic shear frame. Steady state solution.
- Figure 3.1 - Three-dimensional shear frame.
- Figure 3.2 - Moment and shear yield profiles of j^{th} column; normality rule.
- Figure 3.3 - Total shear yield profile and lines of action of forces causing translational collapse of a platform supported on three columns.
- Figure 3.4 - Dynamic loading of three-dimensional shear frame when $C_p = C_G$.
- Figure 3.5 - Yield profiles and principal directions η .
- Figure 3.6 - Response to impulse \dot{u}_0 . General yield profile.
- Figure 3.7 - Response to impulse \dot{u}_0 . Particular example.
- Figure 3.8 - Motion with a "strip" yield profile ($k_y = \infty$).
- Figure 3.9 - Response to periodic loading (rectangular yield profile; both load components in Case II).
- Figure 3.10 - Steady-state velocities for loading in Figure 3.9.
- Figure 3.11 - Response to periodic loading (rectangular yield profile: x-component in Case I, y-component in Case II).
- Figure 3.12 - Steady-state velocities for loading in Figure 3.11.

- Figure 3.13 - Determination of sign of steady-state movement of L and U .
- Figure 4.1 - Shear frame under horizontal and vertical loads.
- Figure 4.2 - Motion of frame subjected to horizontal loads $\xi(t)$ and constant vertical forces.
- Figure 4.3 - Response of frame subjected to constant gravity forces and a horizontal impulse: a) velocity of deformation \dot{u} vs. time t and initial velocity \dot{u}_0 ; b) initial velocity \dot{u}_0 vs. total response time t_f .
- Figure 4.4 - Frame subjected to periodic horizontal load and constant vertical forces; determination of n^{th} cycle of response.
- Figure 4.5 - Bounds to the critical number of cycles n_c : a) Case I; b) Case II.
- Figure 4.6 - Final cycle of loading.
- Figure 4.7 - Cycle of loading with zero effective strength.
- Figure 4.8 - Approximate lower bound to the critical number of cycles.

Unyielded



Yielded

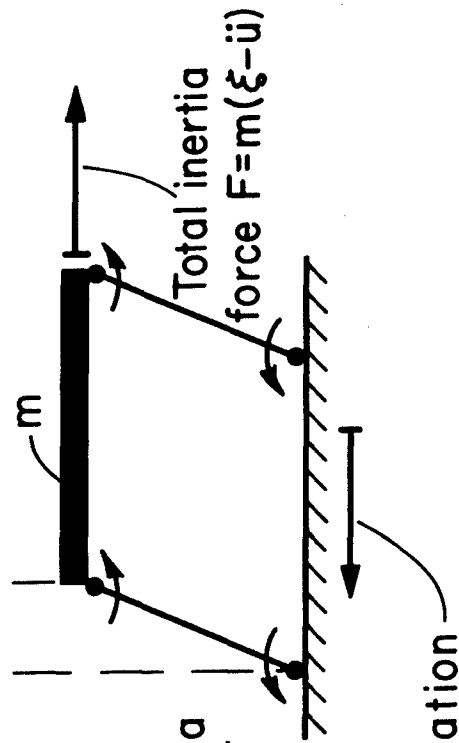
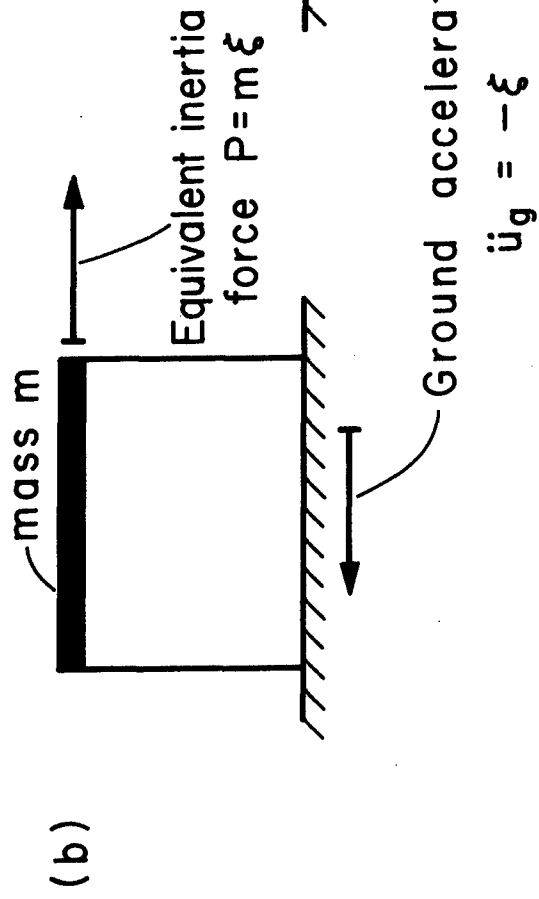
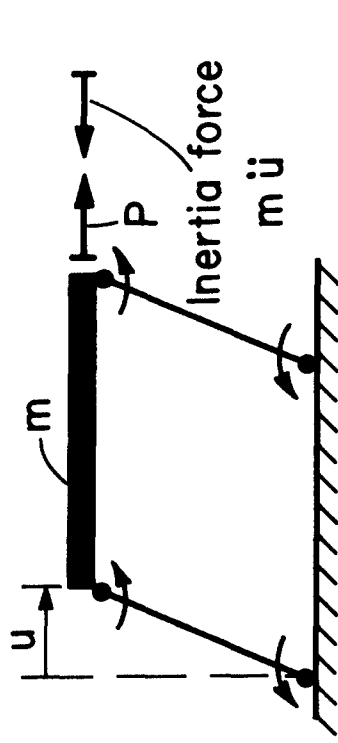


FIG. 1.1

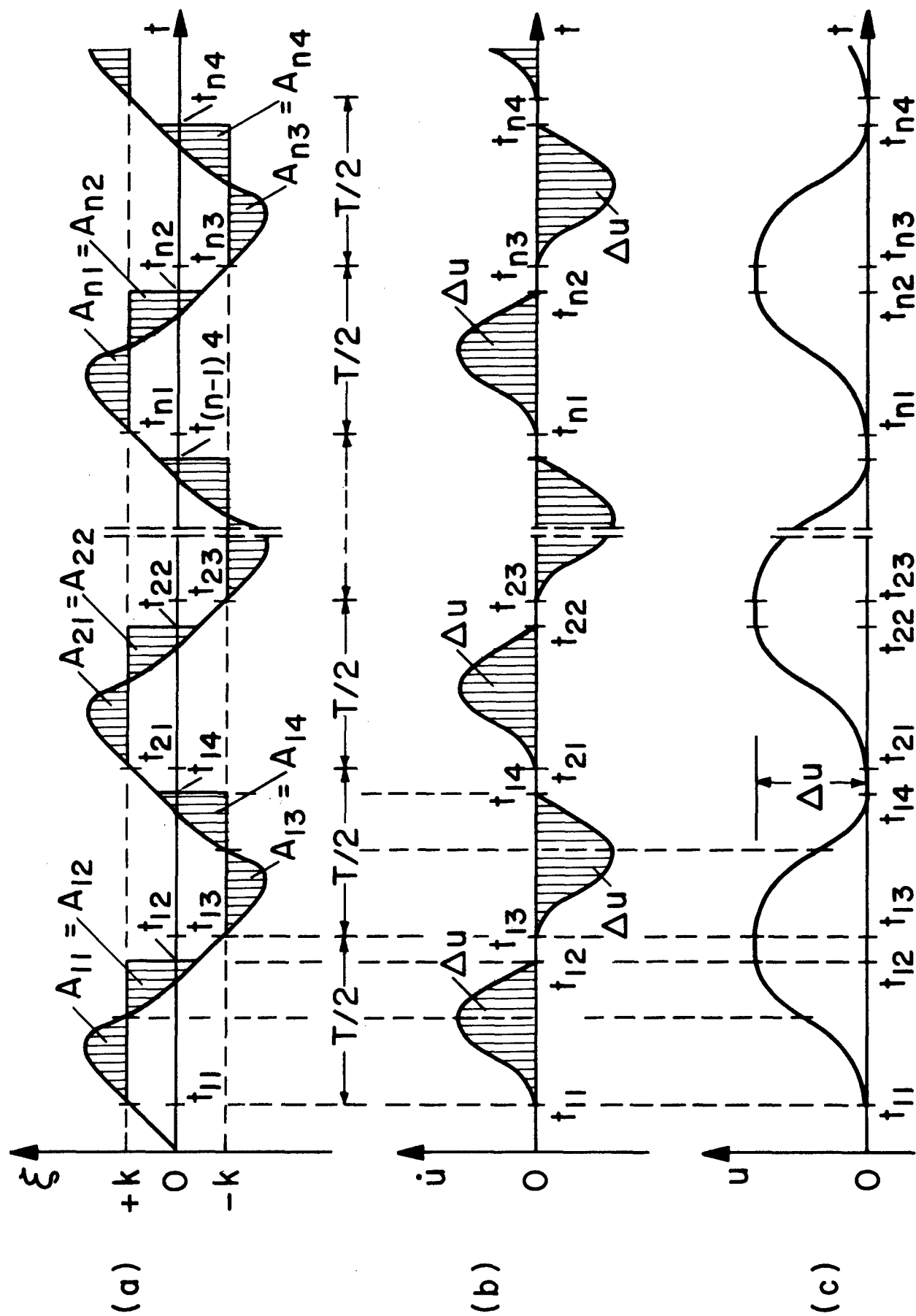


FIG. 1.2

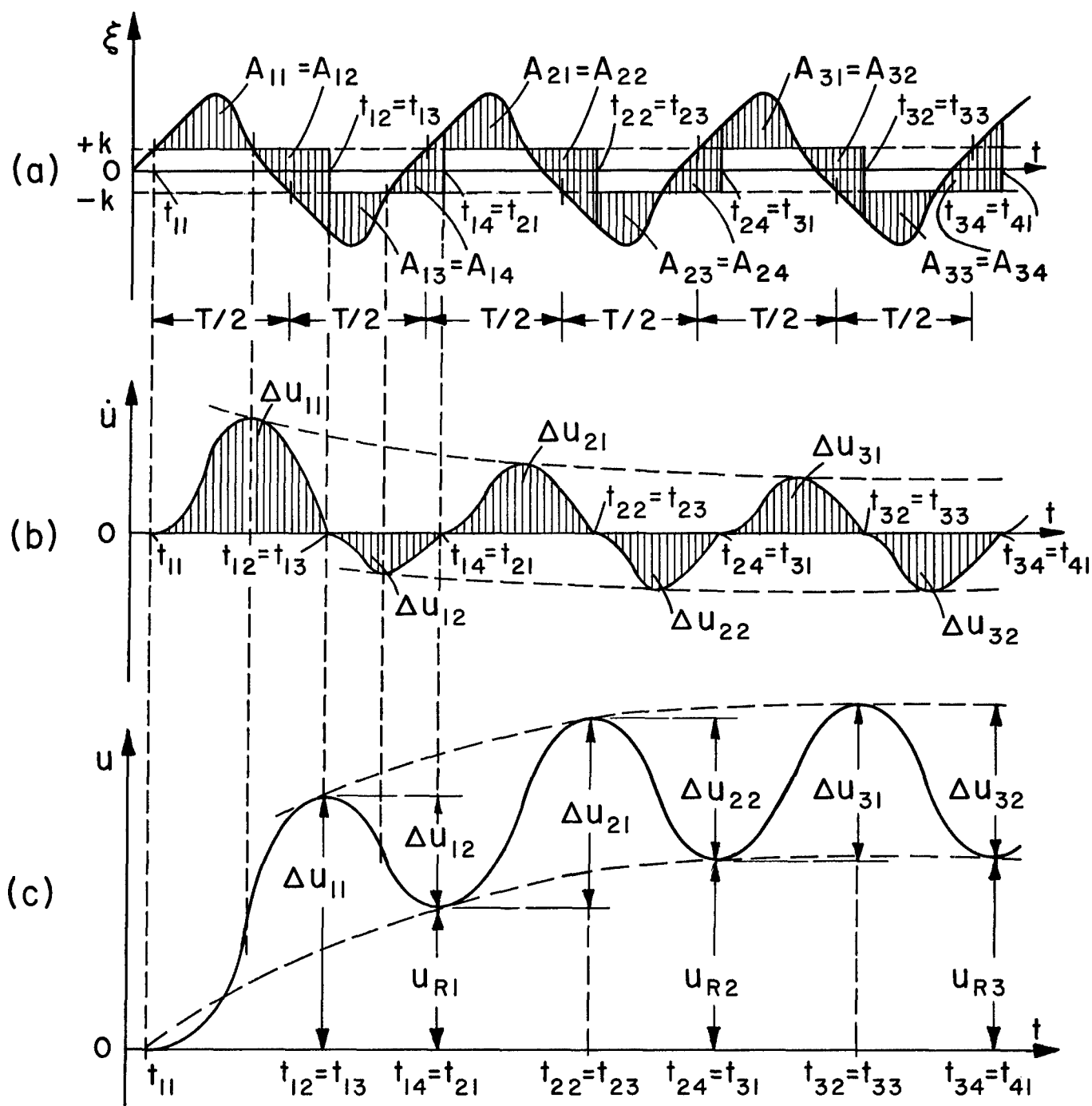


FIG. 1.3

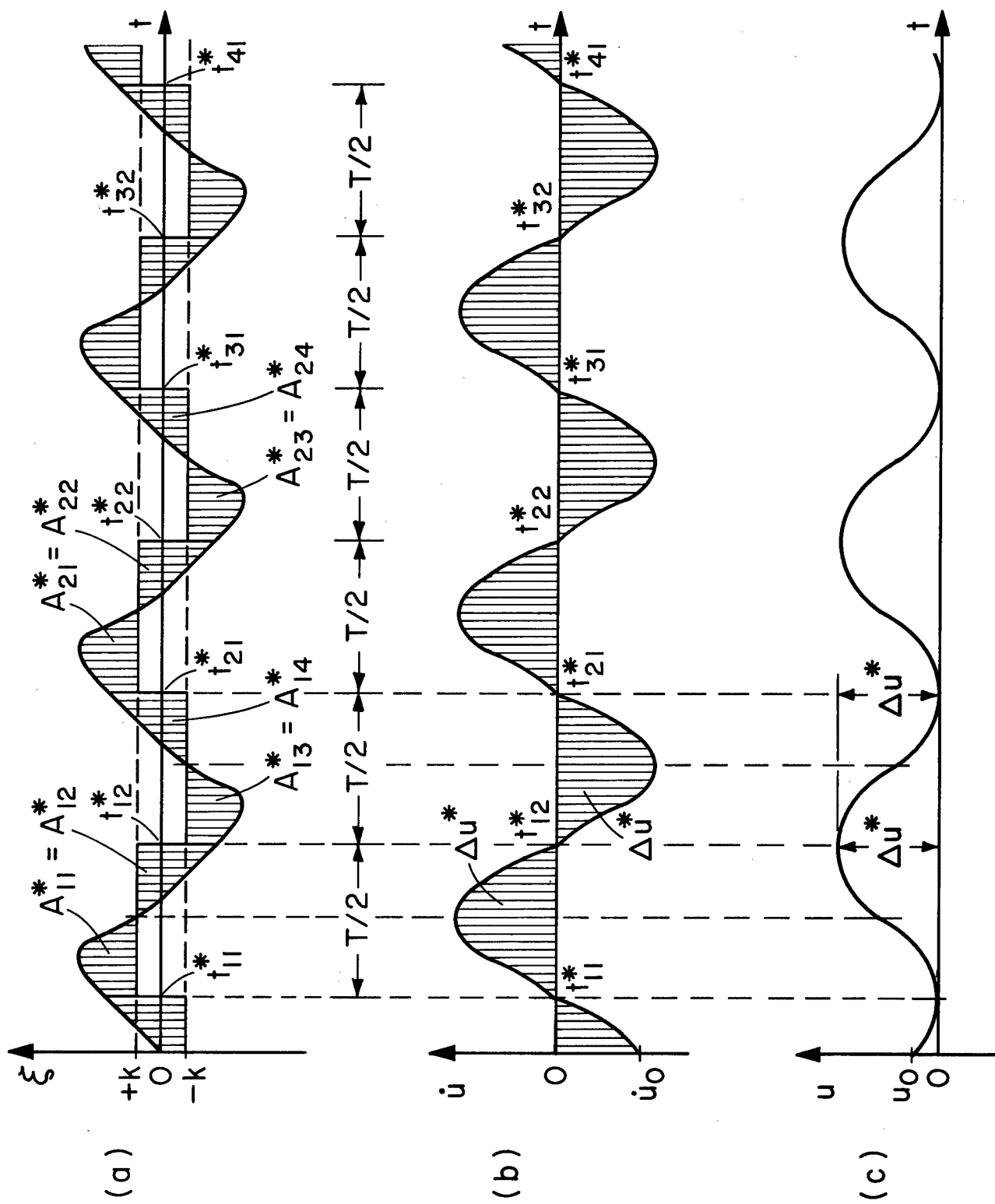


FIG. 1.4

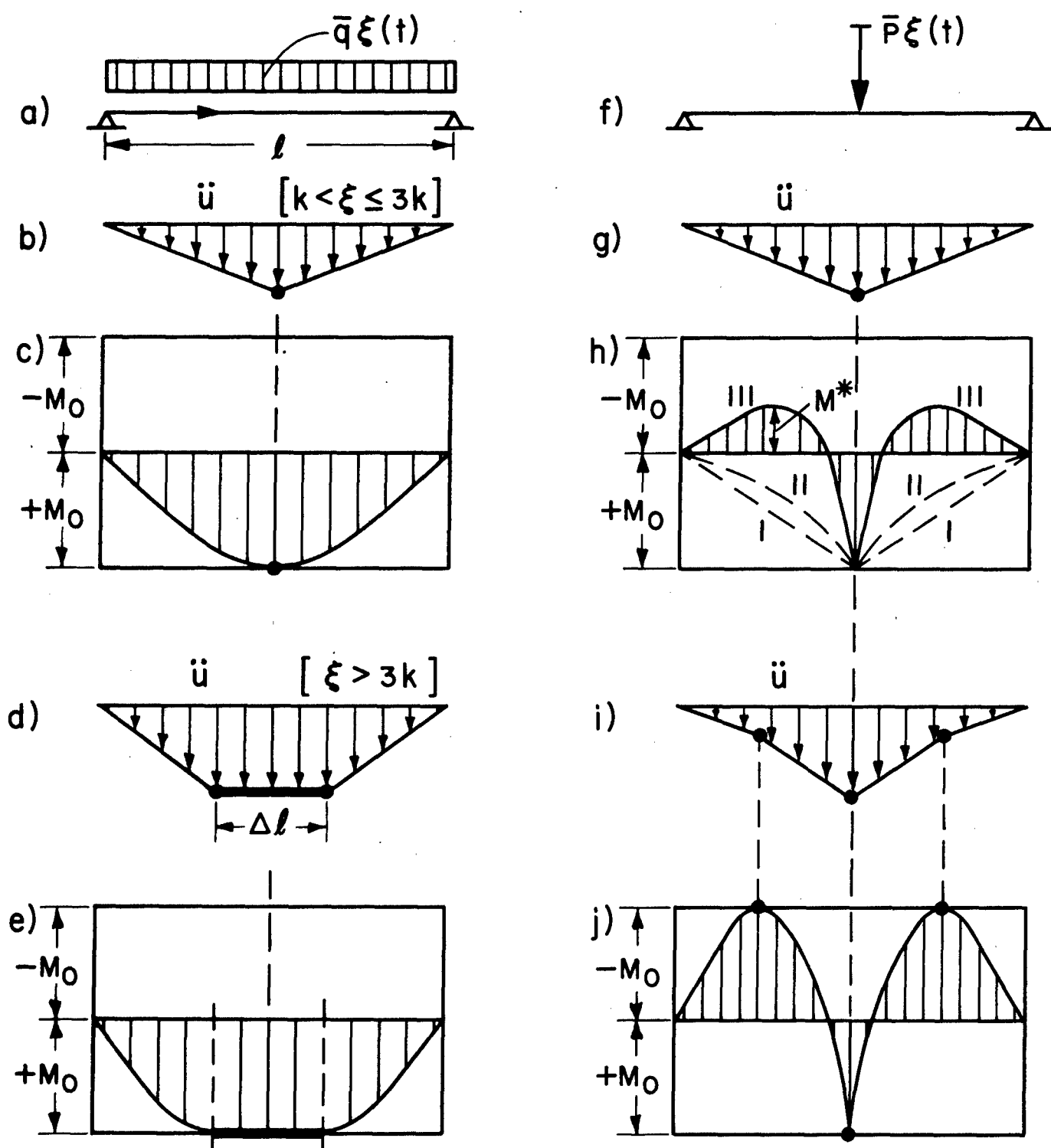


FIG. 2.1

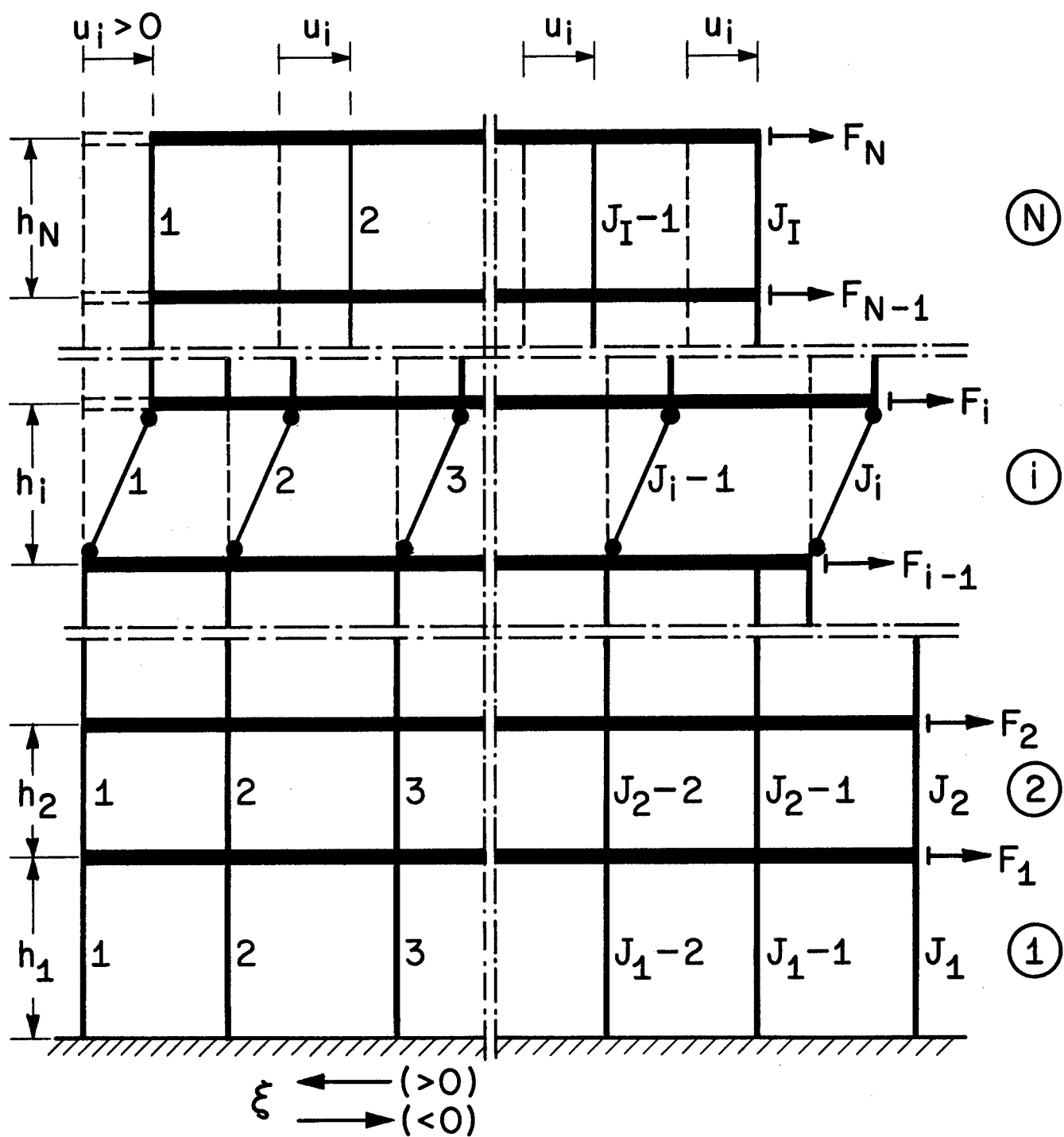


FIG. 2.2

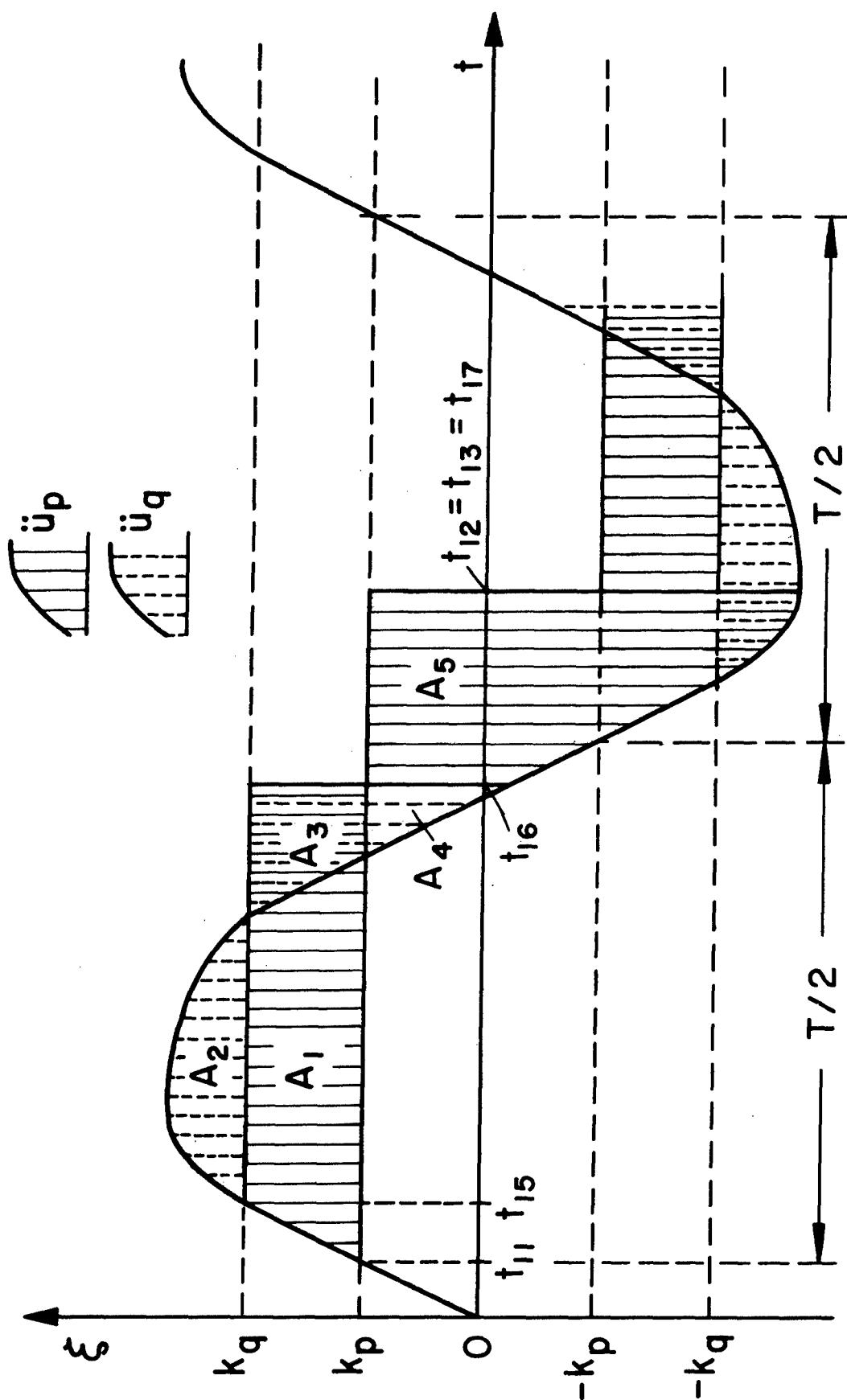


FIG. 2.3

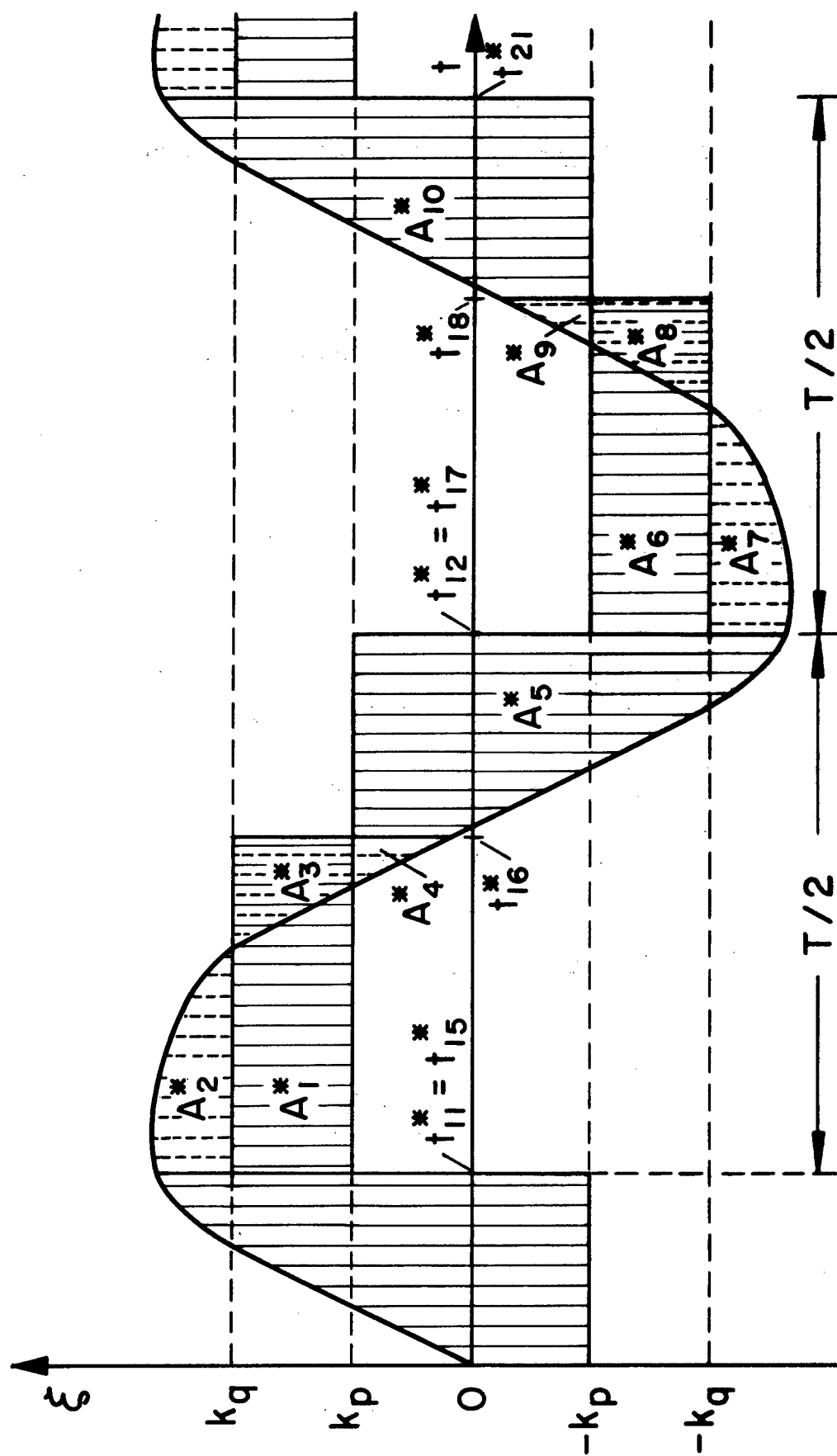


FIG. 2.4

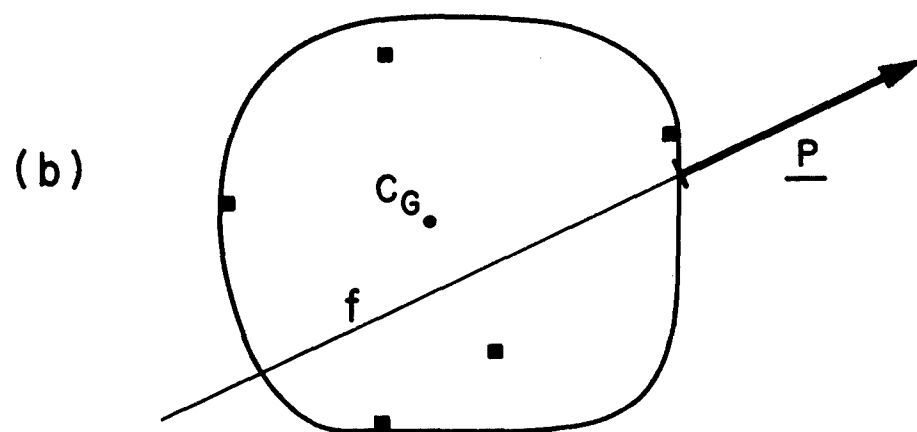
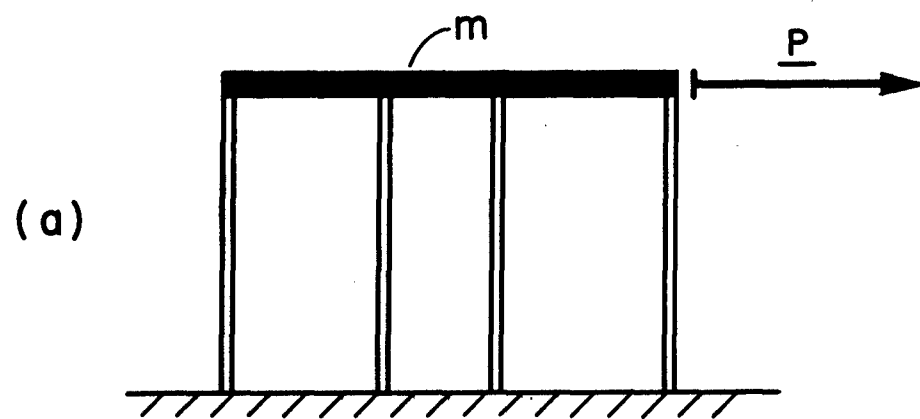


FIG. 3.1

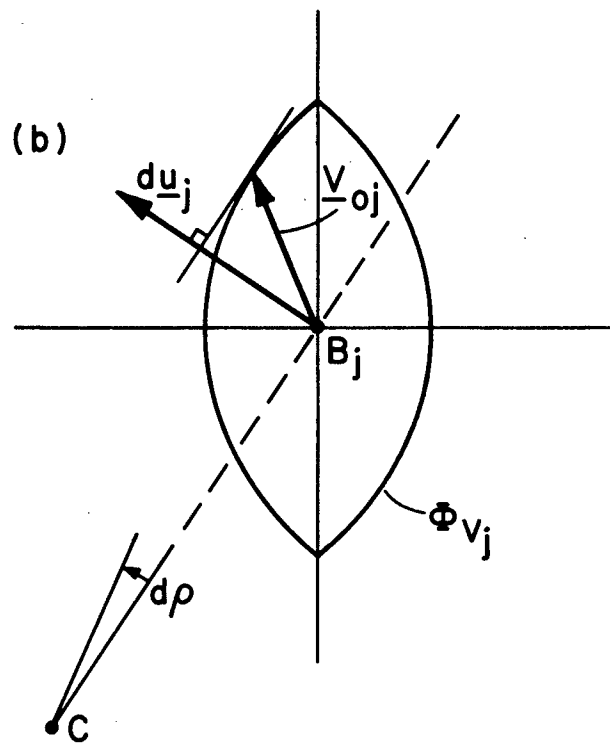
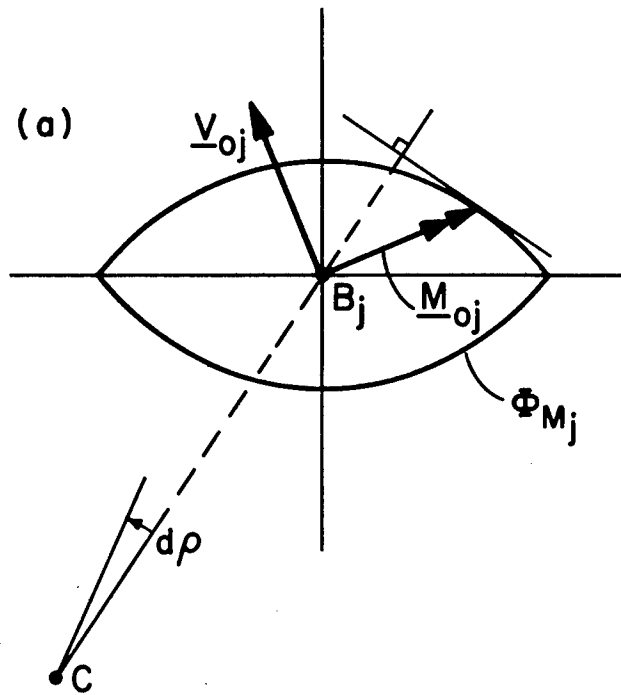


FIG. 3.2

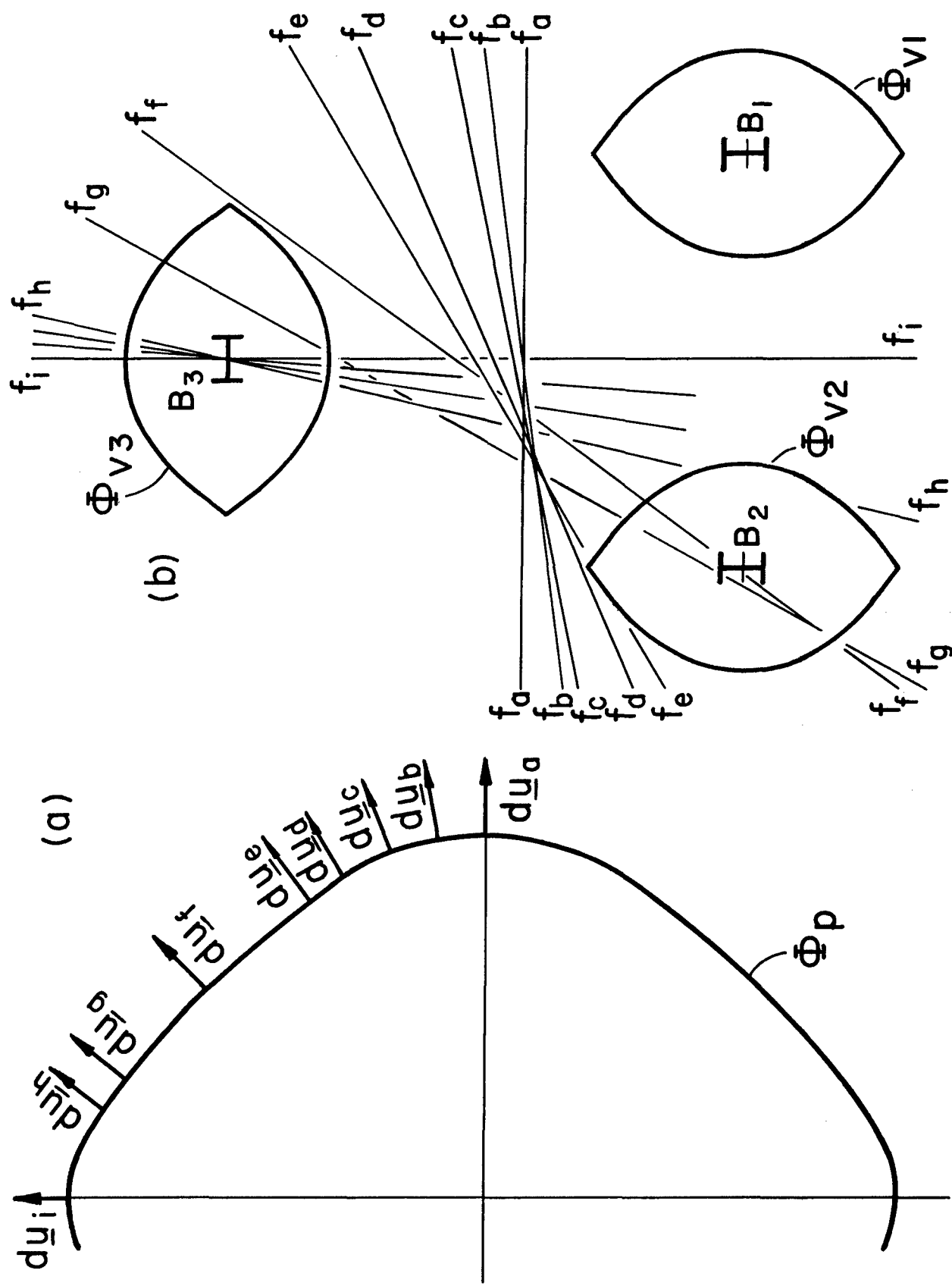


FIG. 3.3

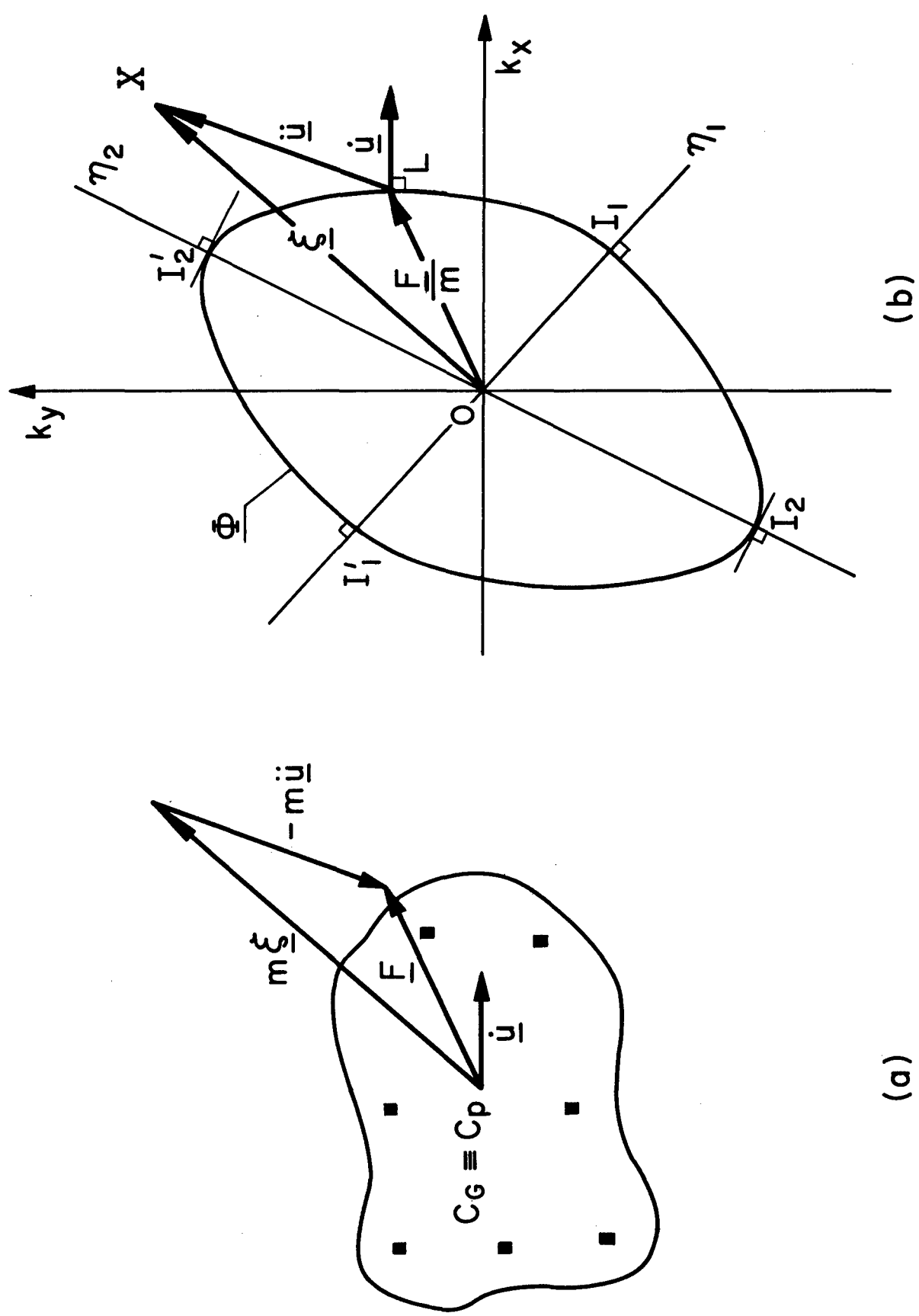


FIG. 3.4

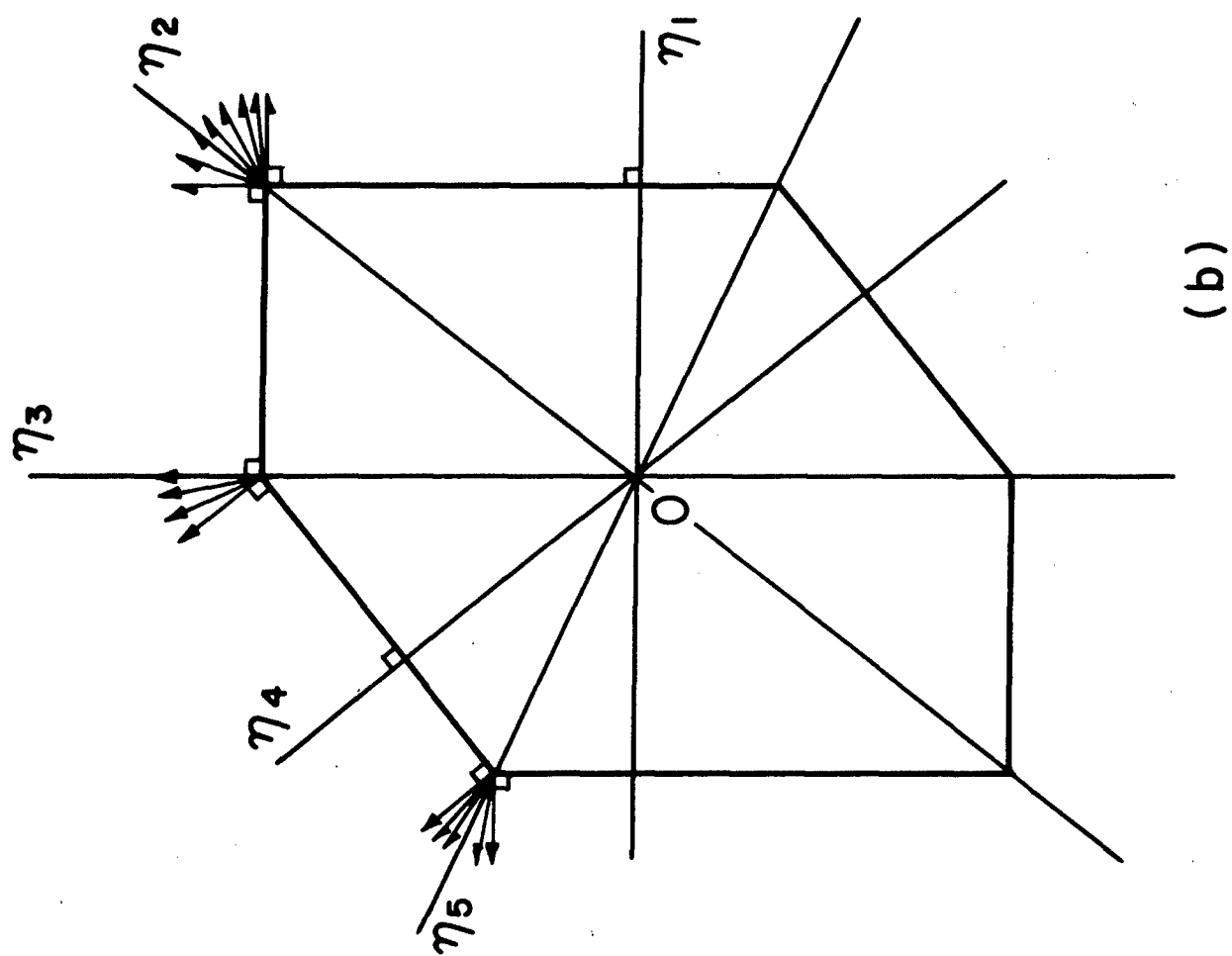
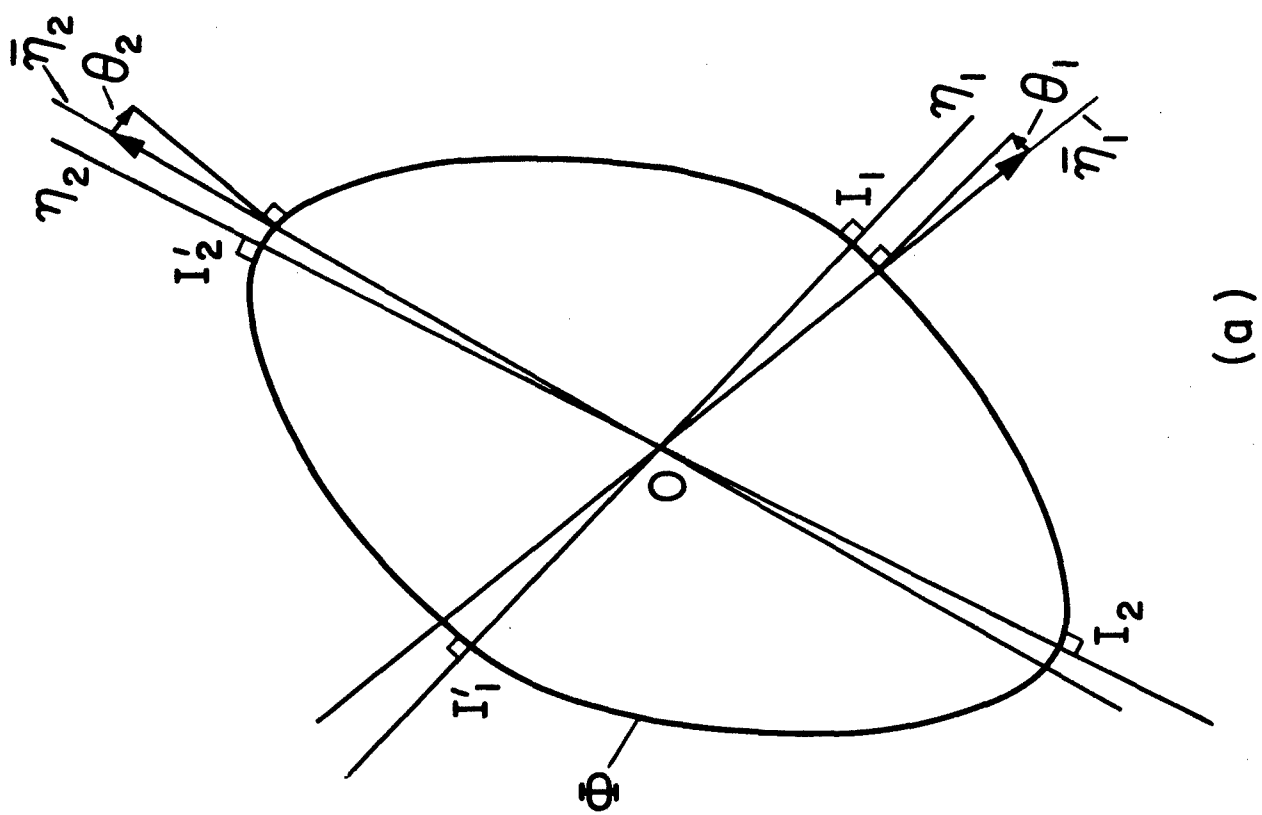


FIG. 3.5

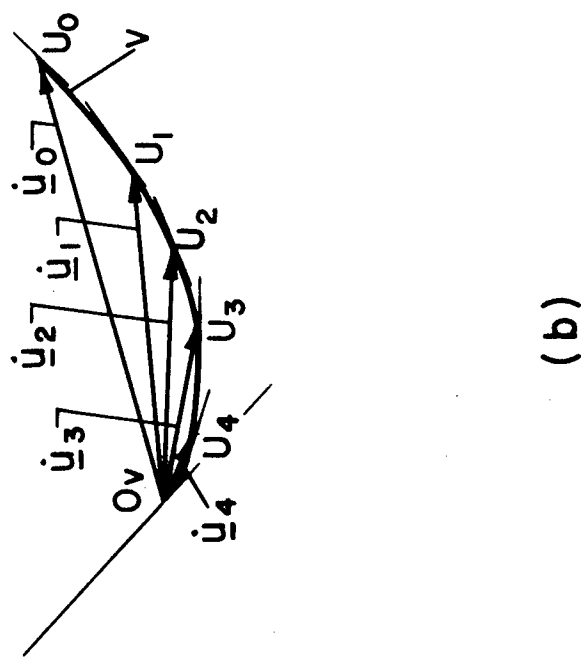
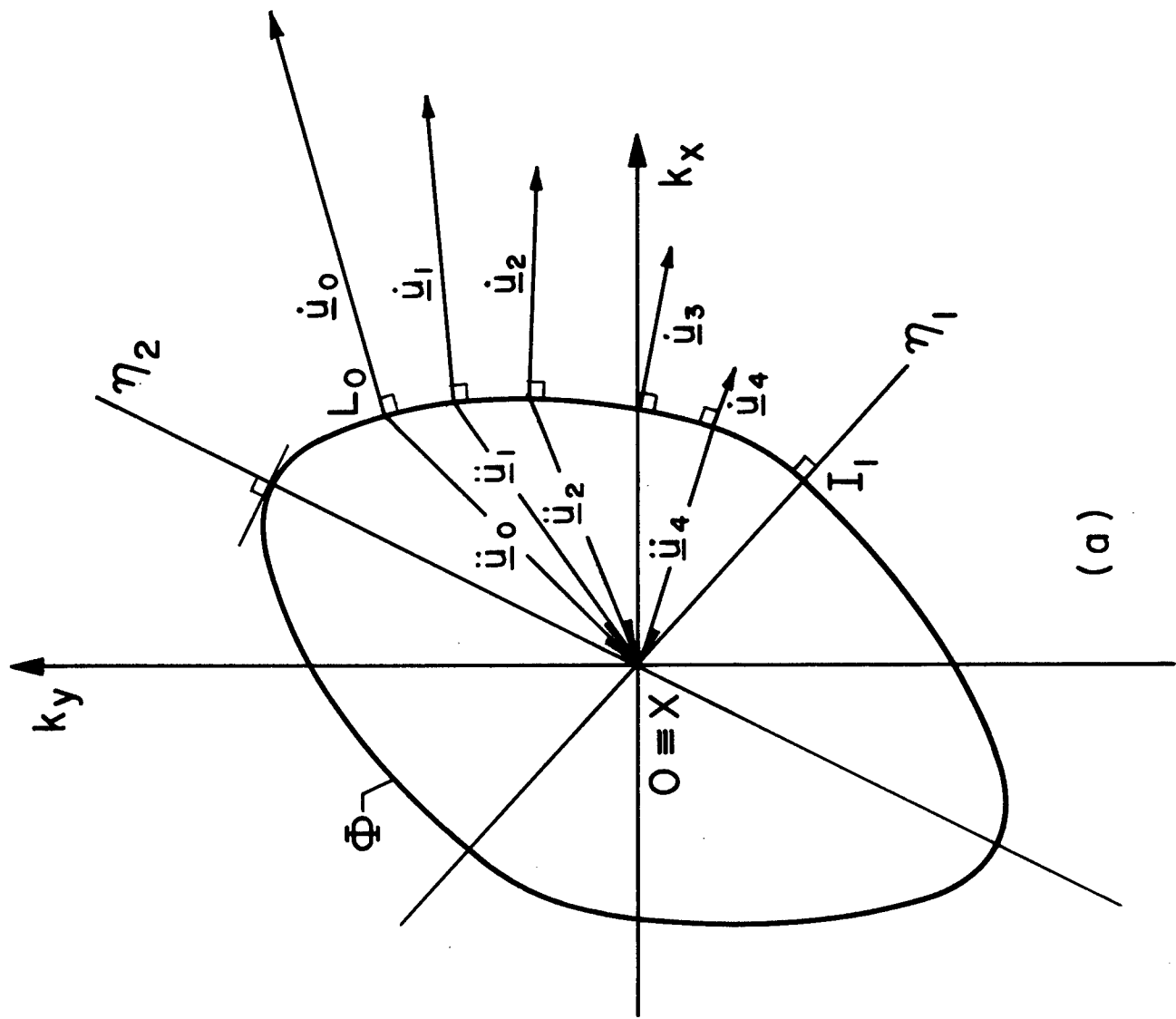


FIG. 3.6

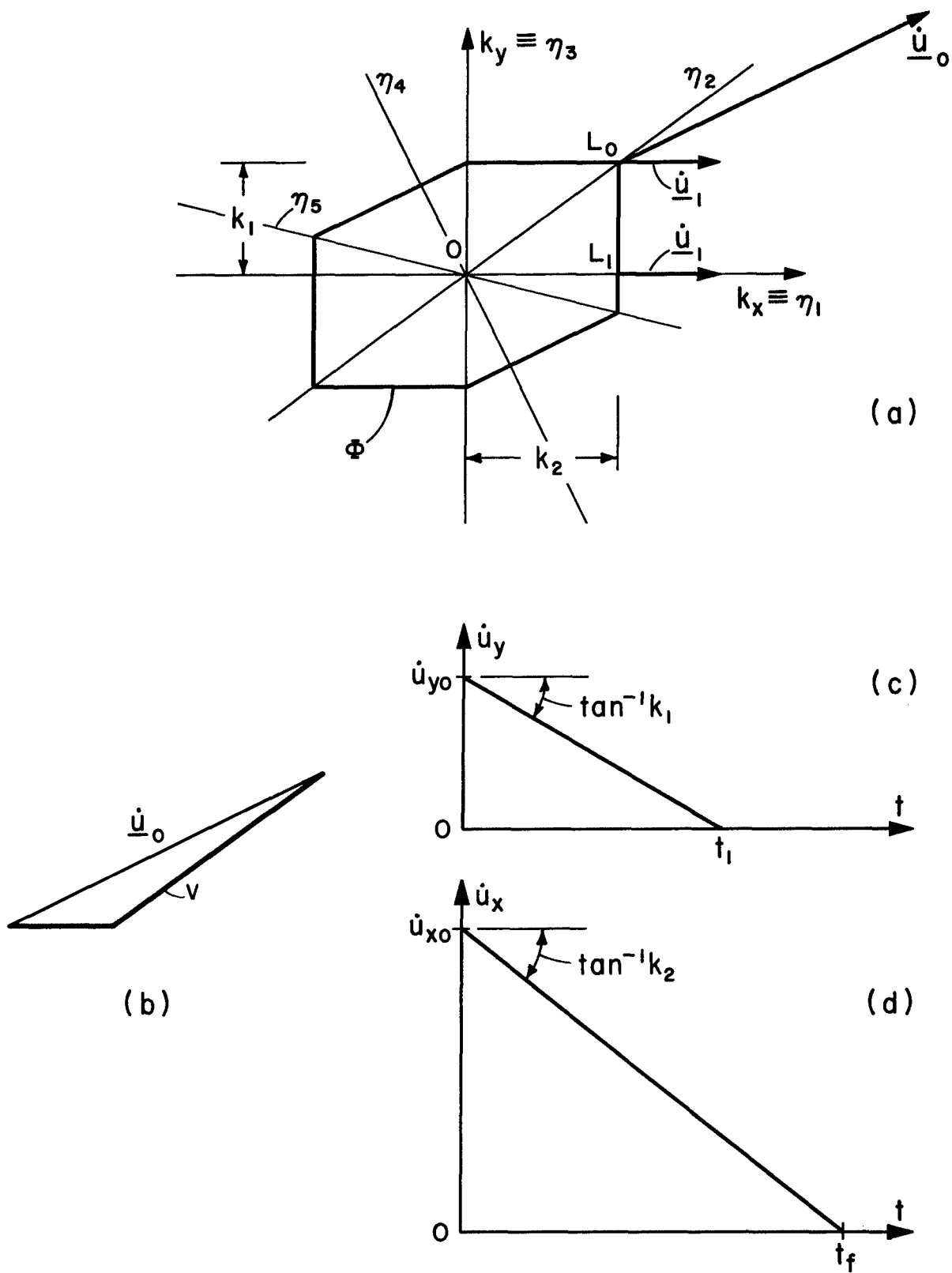


FIG. 3.7

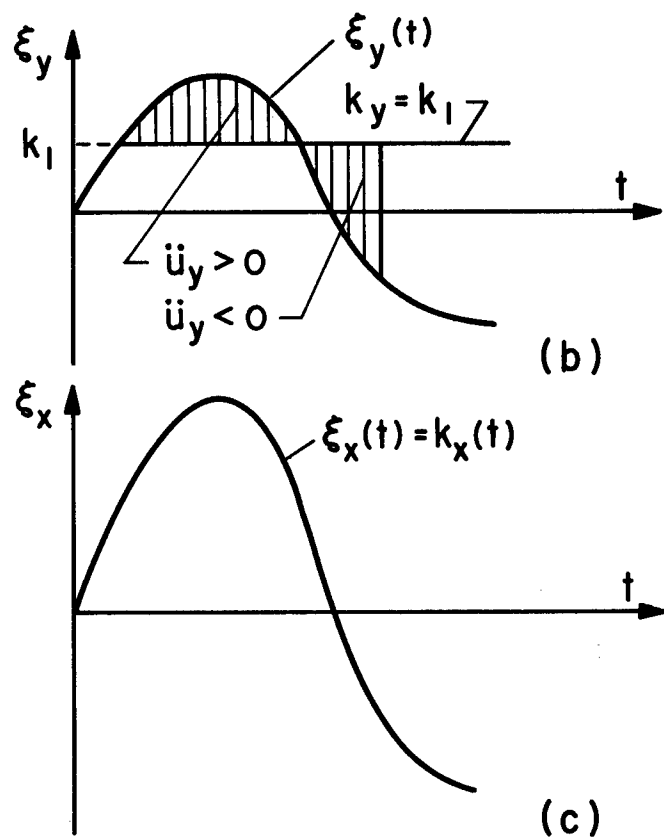
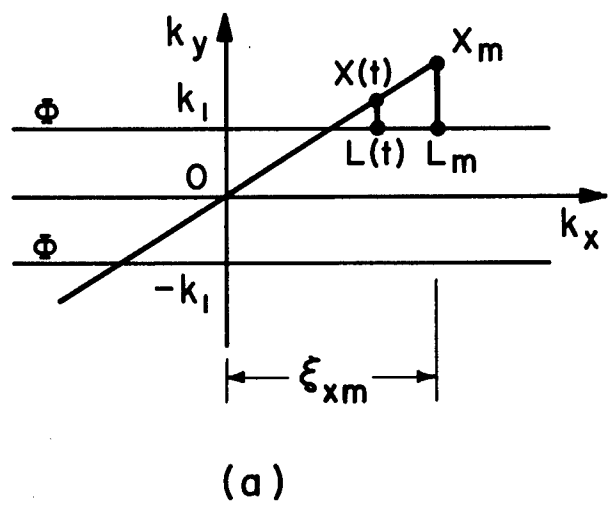


FIG. 3.8

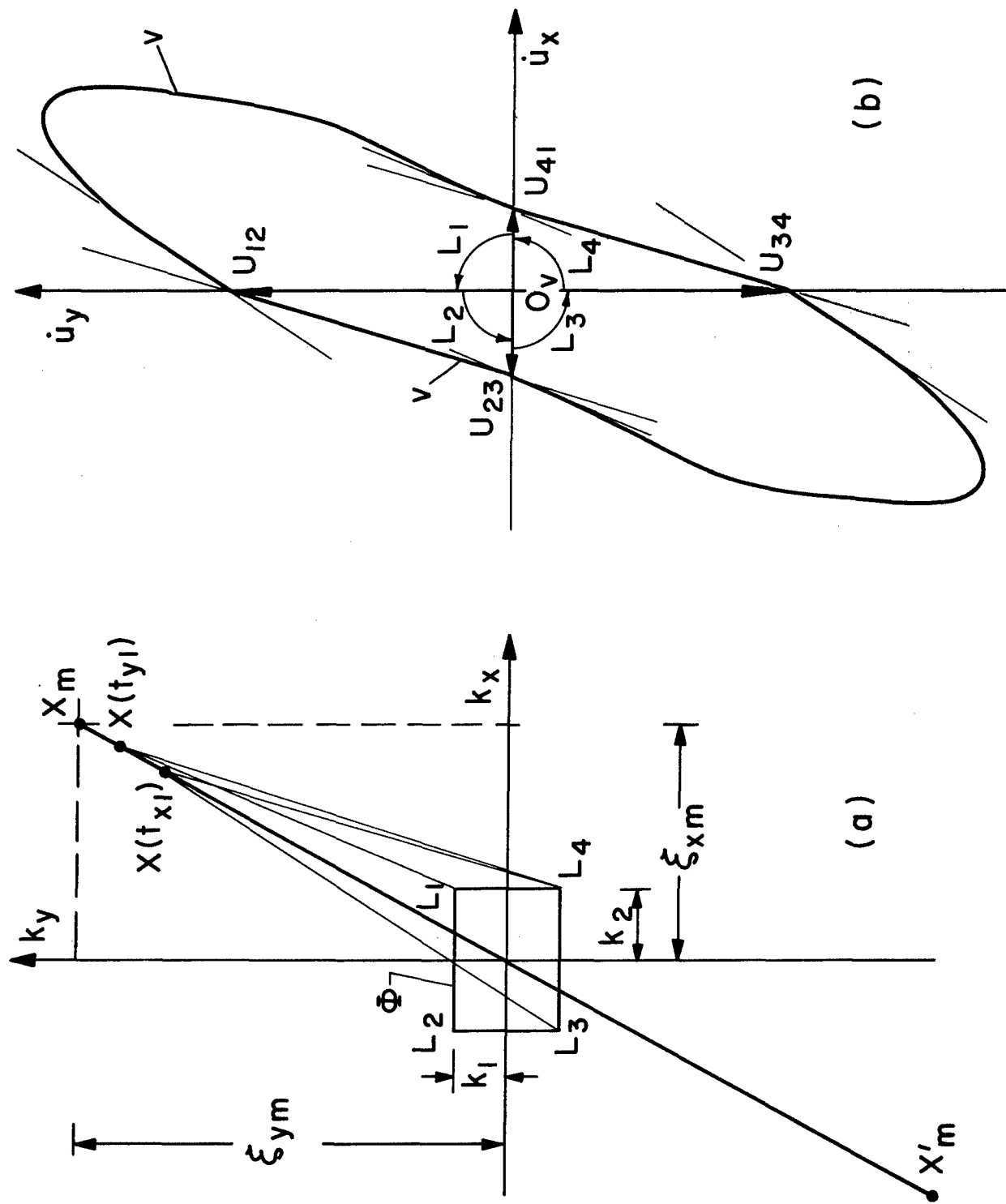


FIG. 3.9

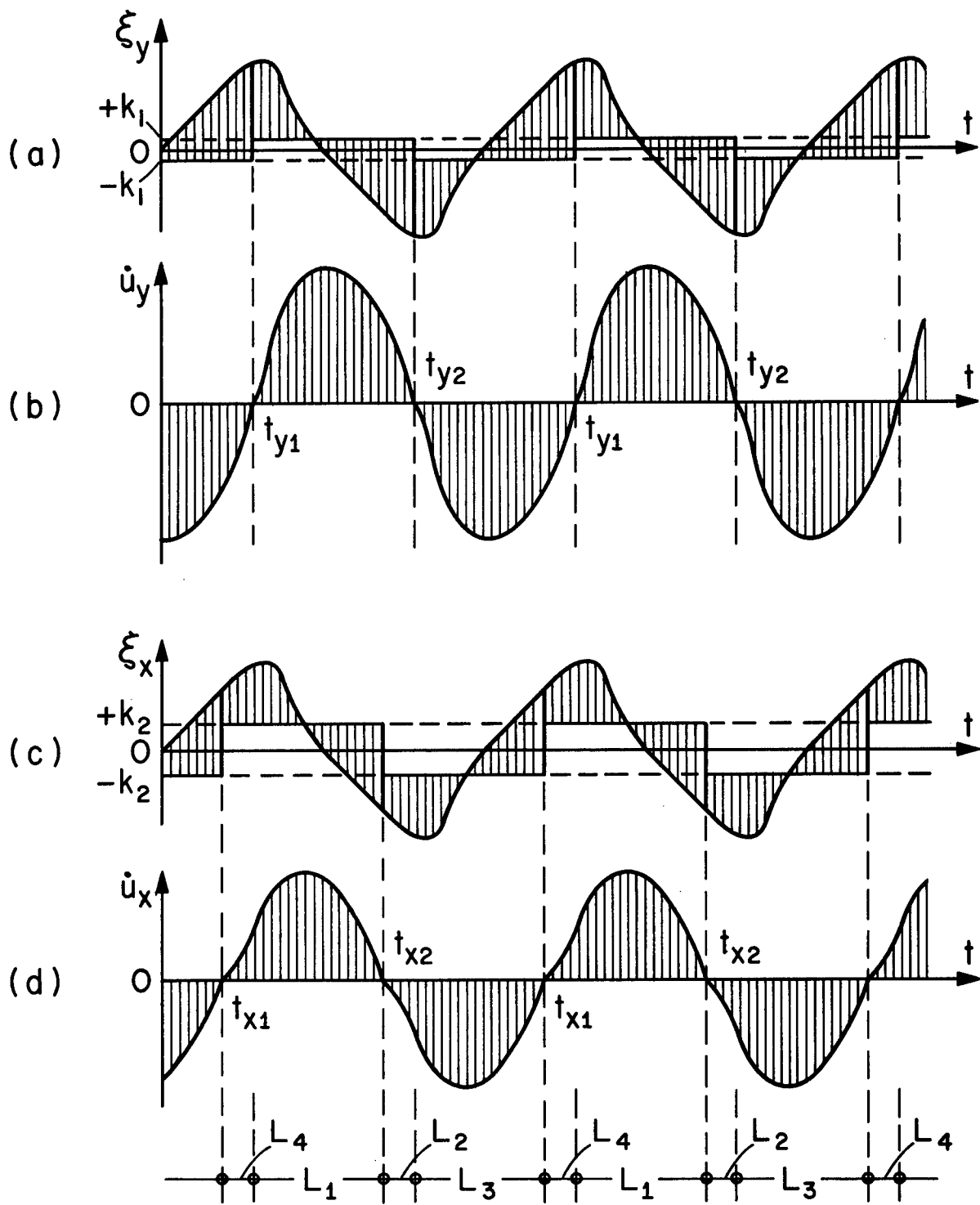


FIG. 3.10

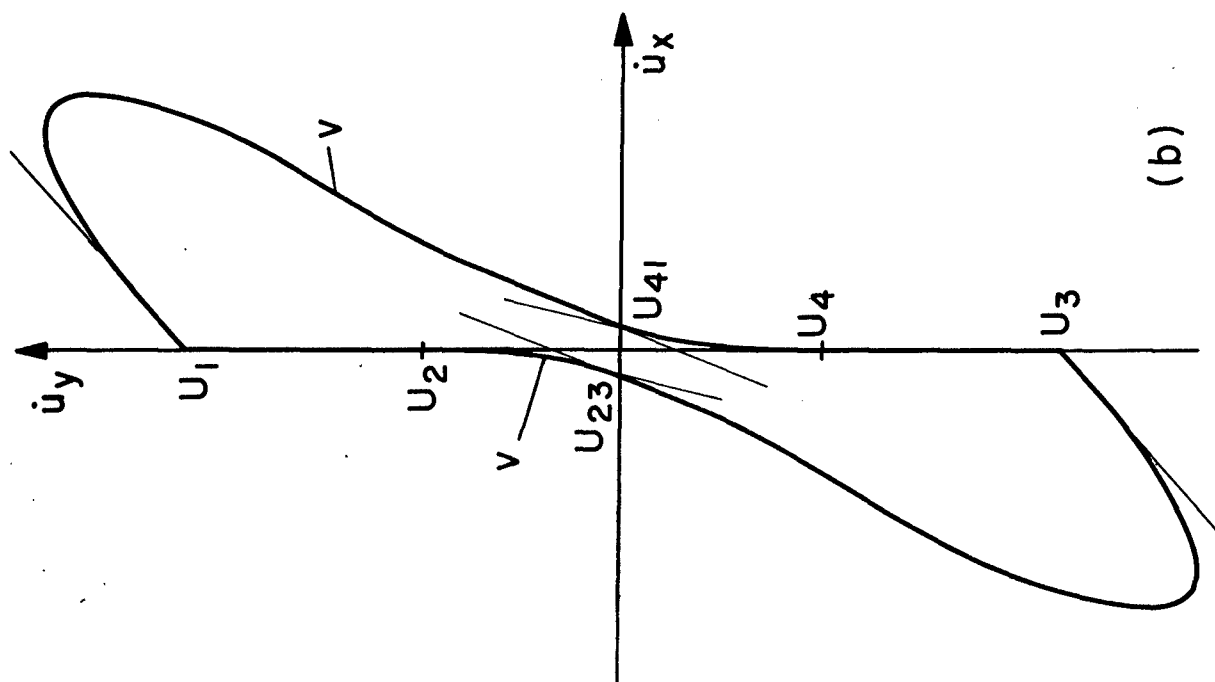
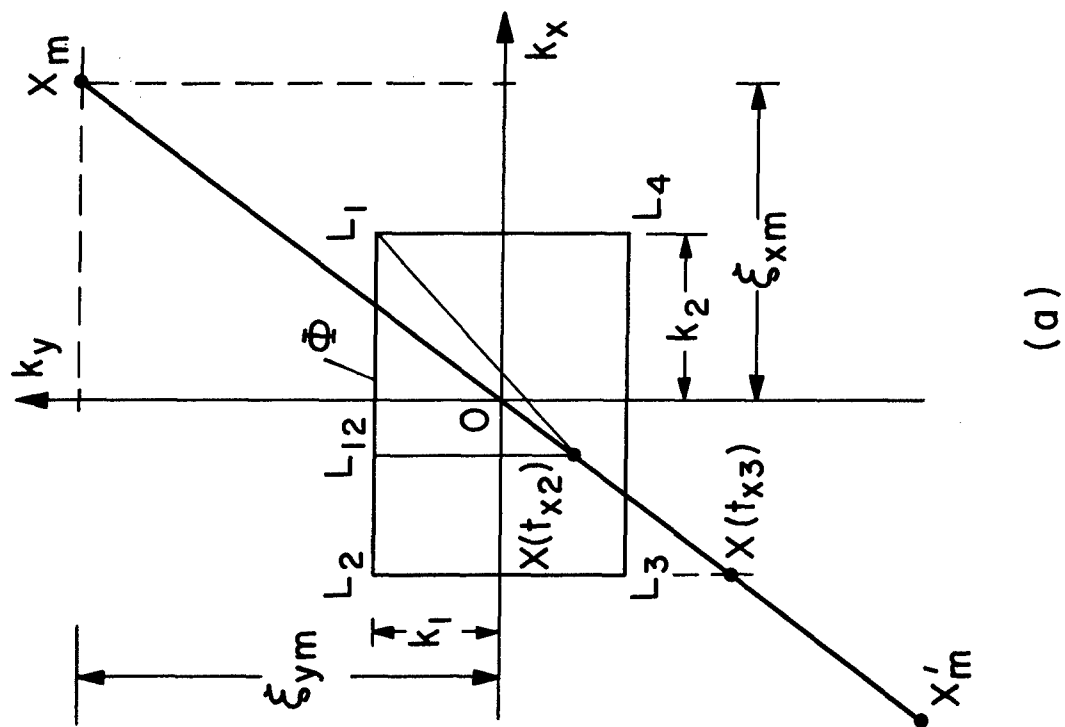


FIG. 3.11

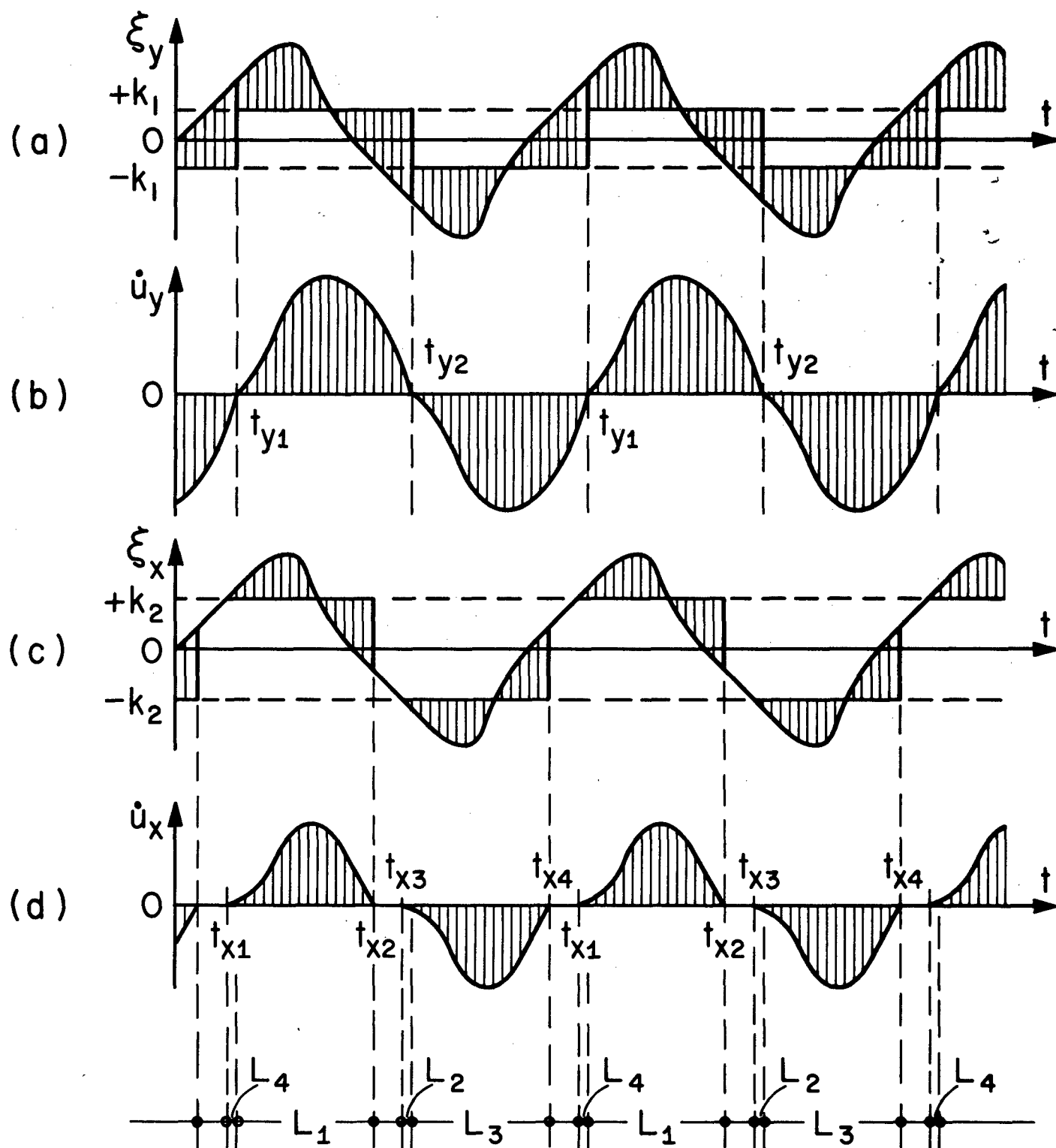


FIG. 3.12

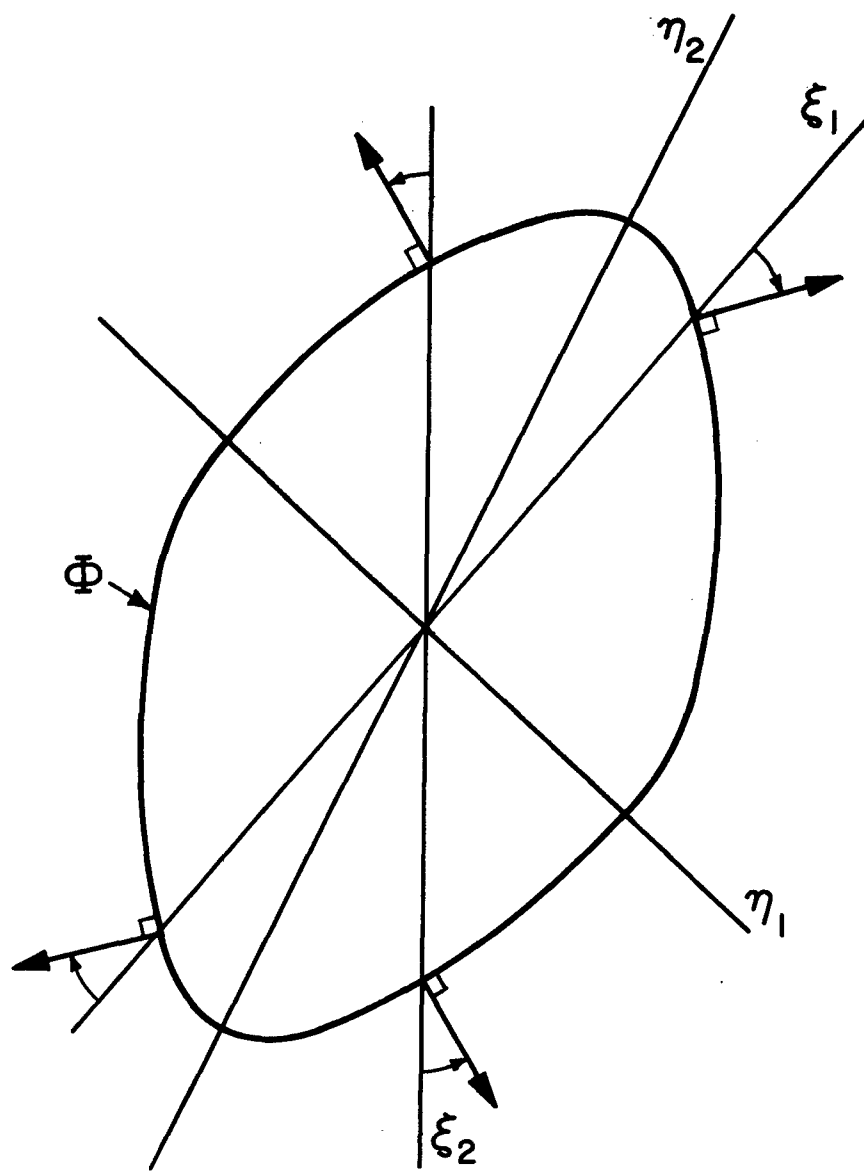


FIG. 3.13

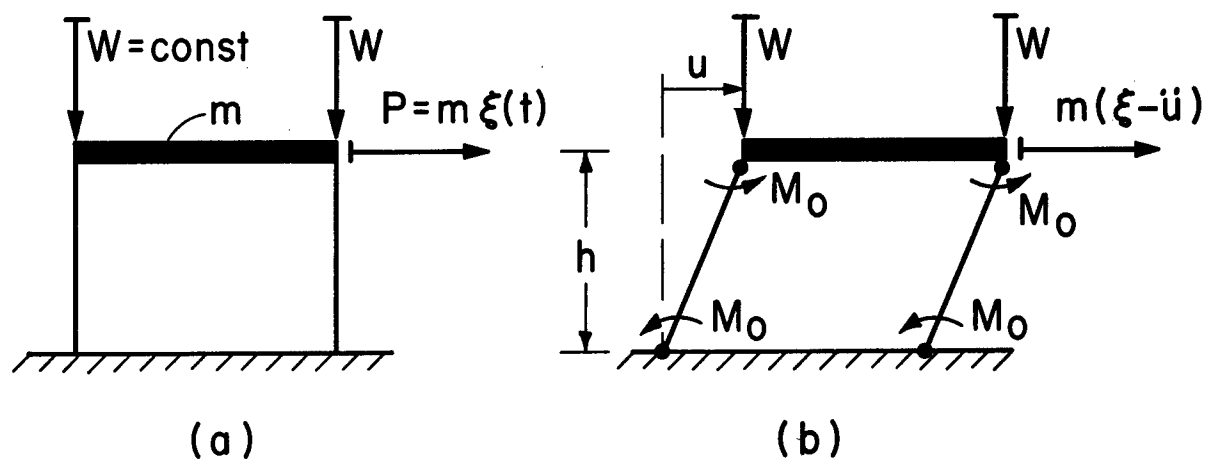


FIG. 4.1

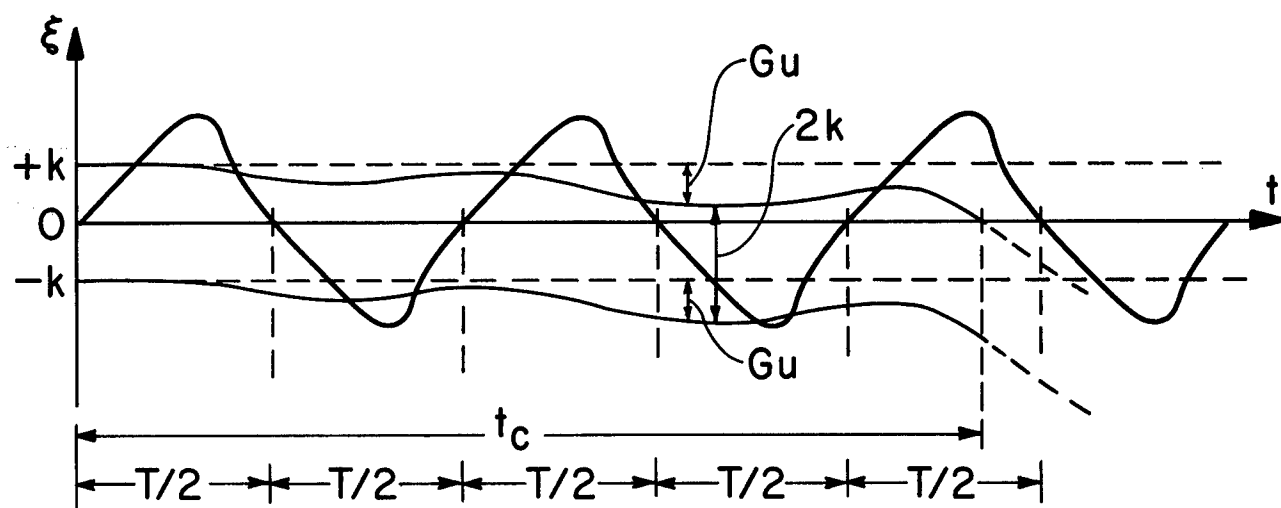
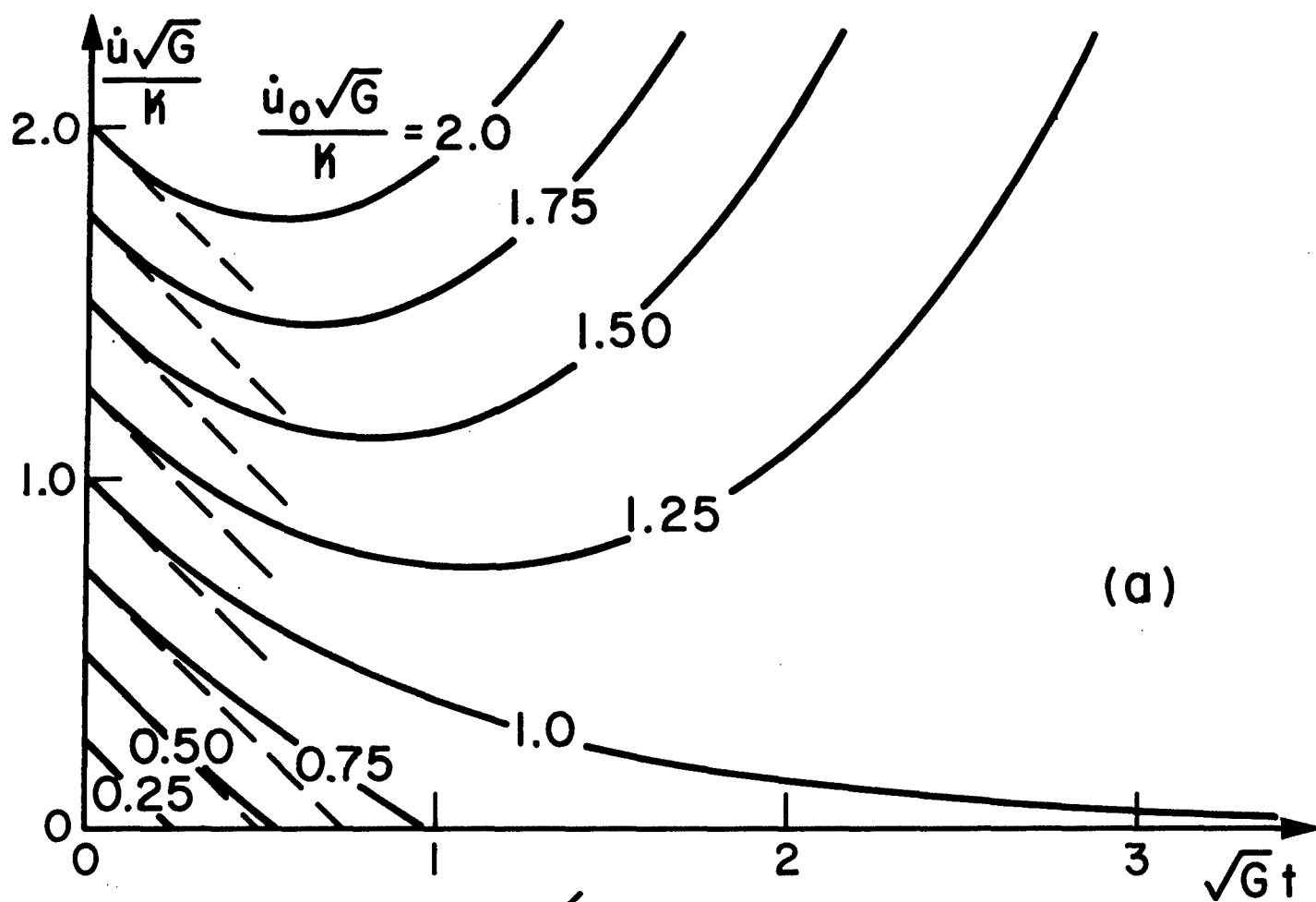
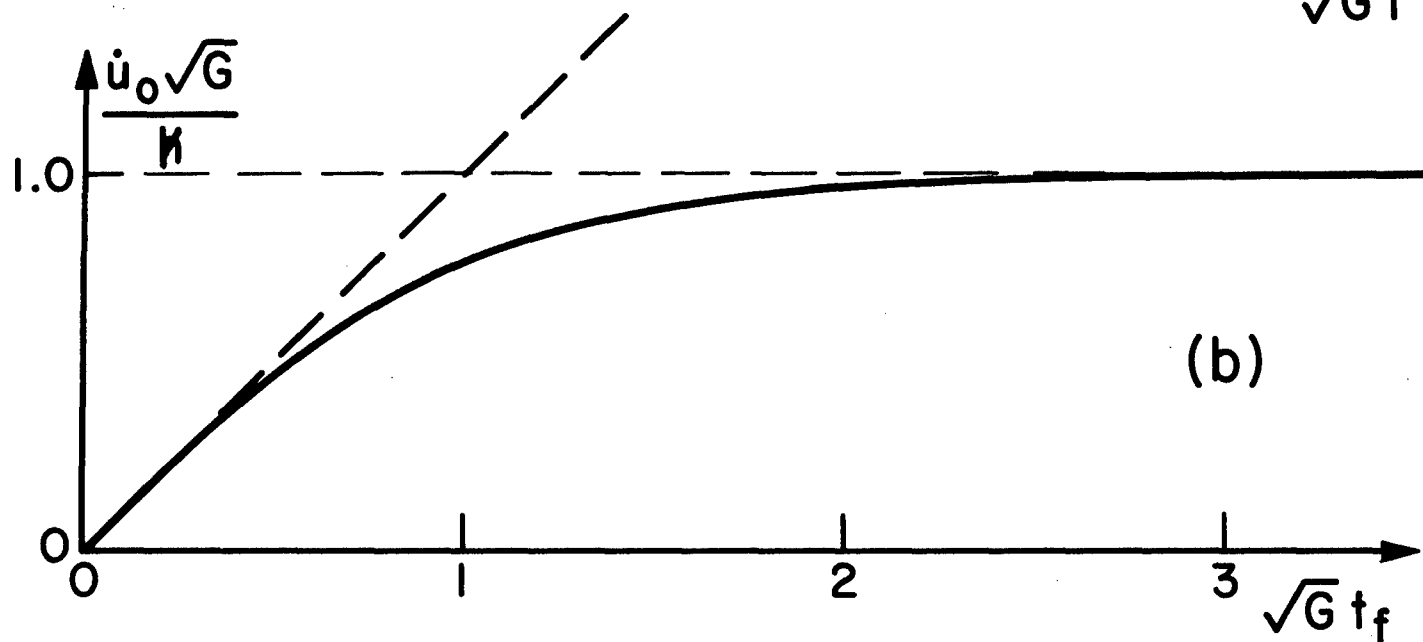


FIG. 4.2



(a)



(b)

FIG. 4.3

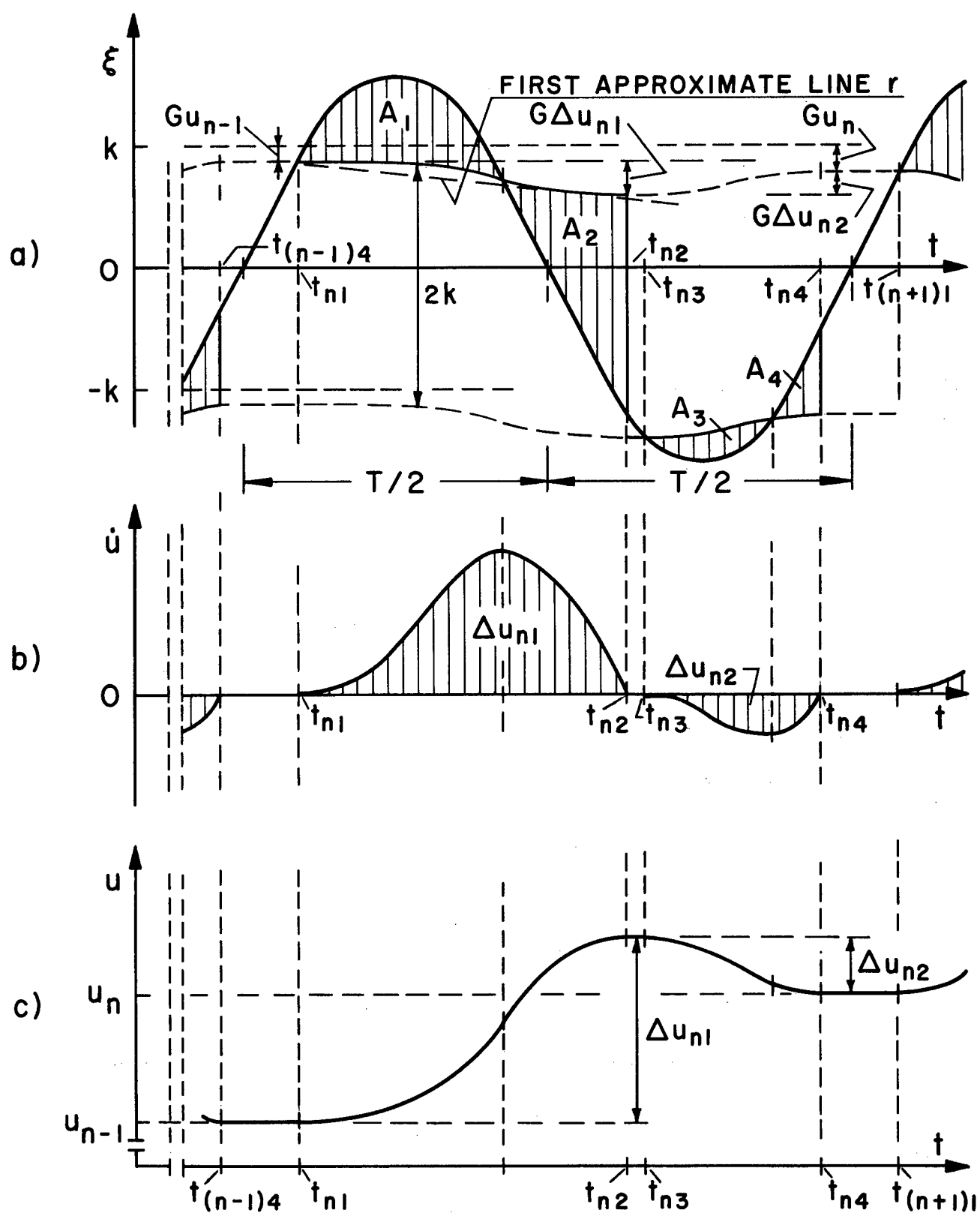


FIG. 4.4

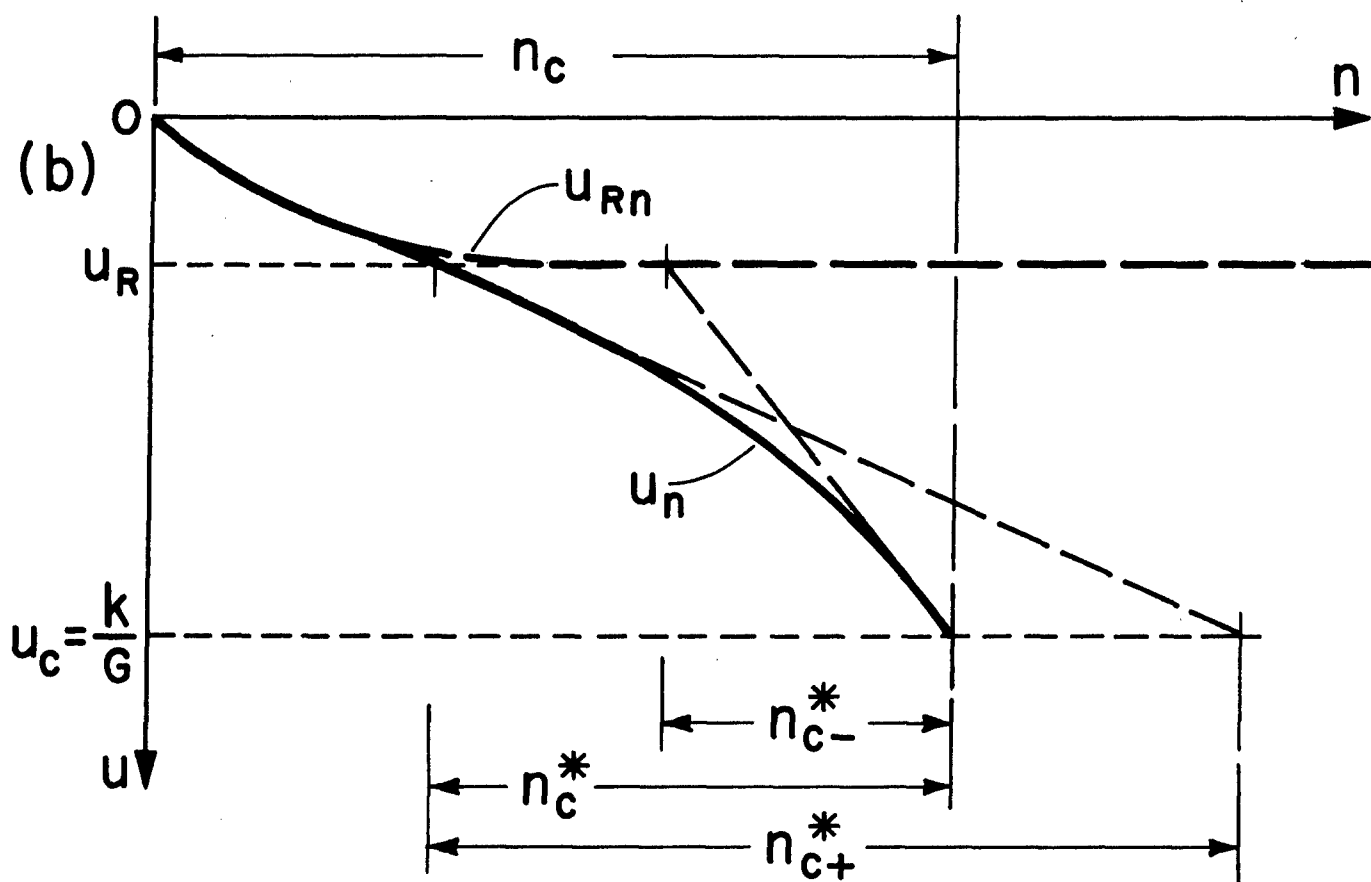
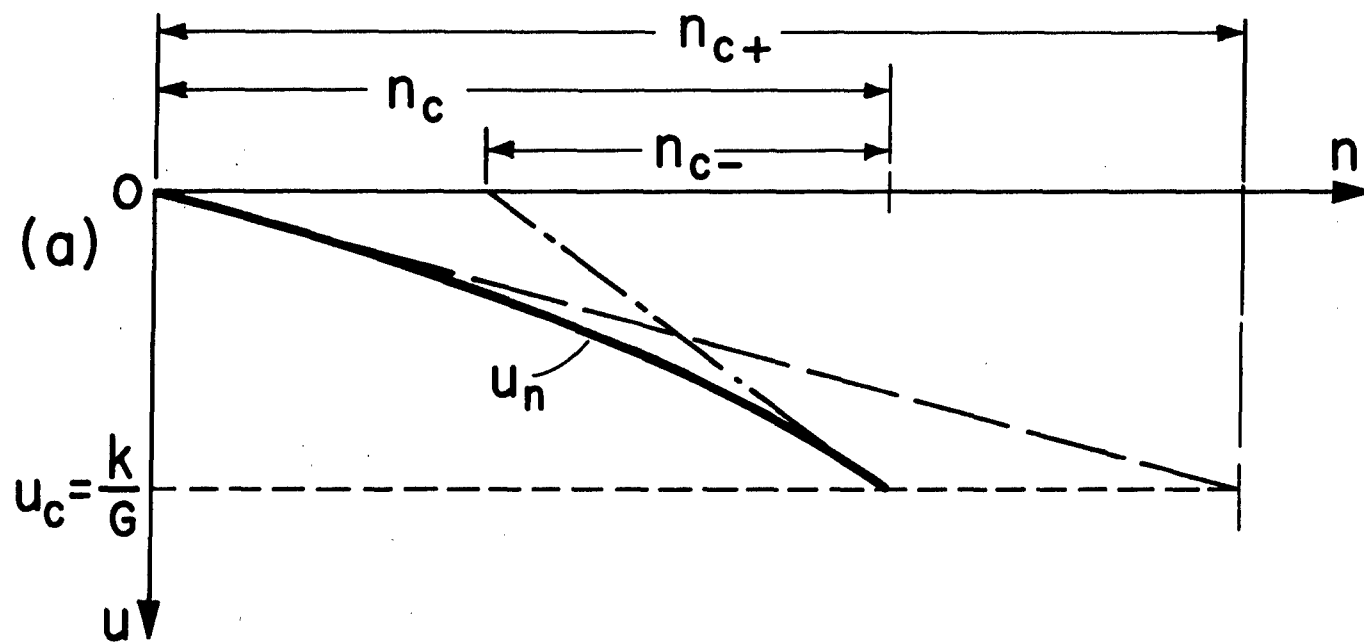


FIG. 4.5

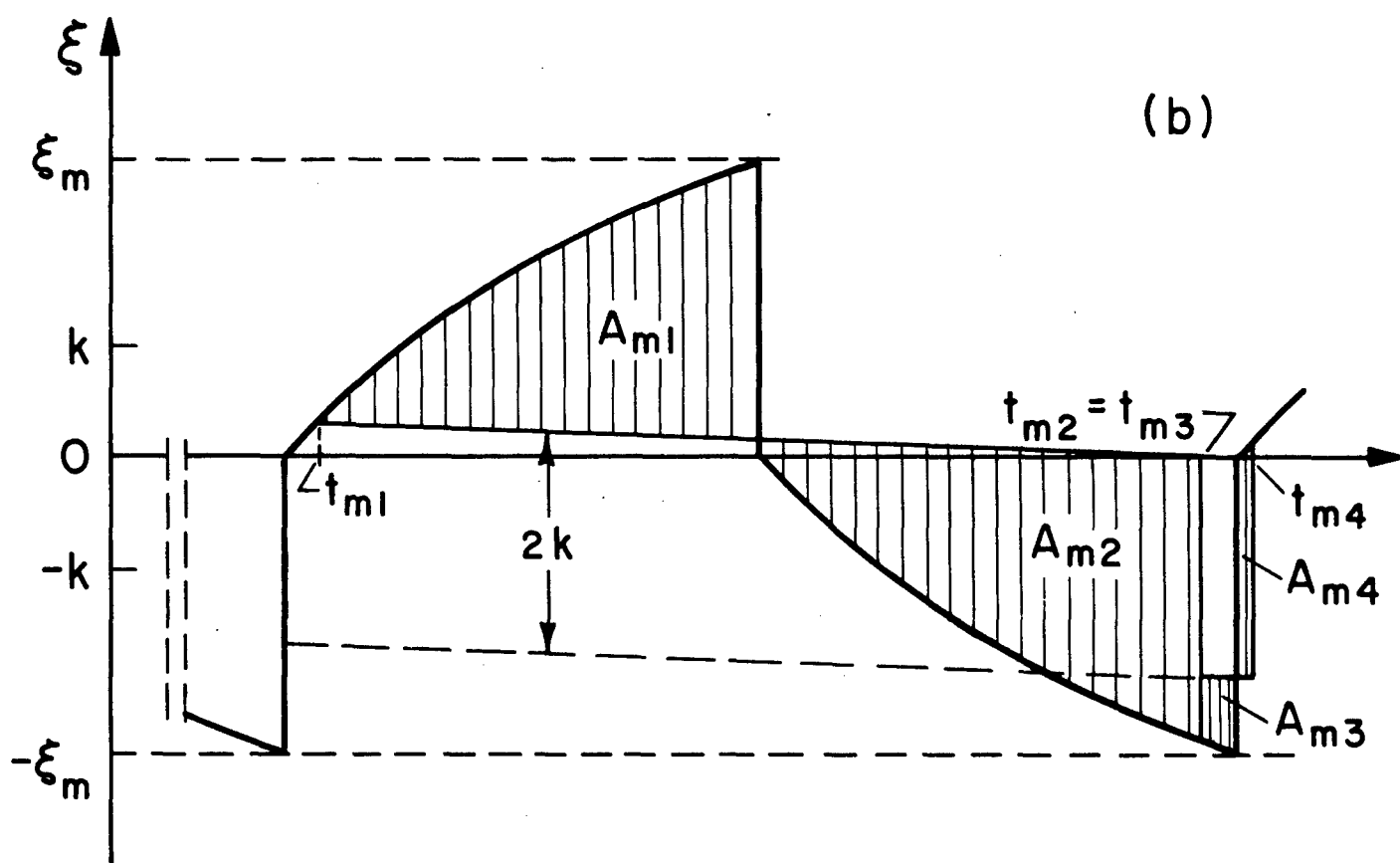
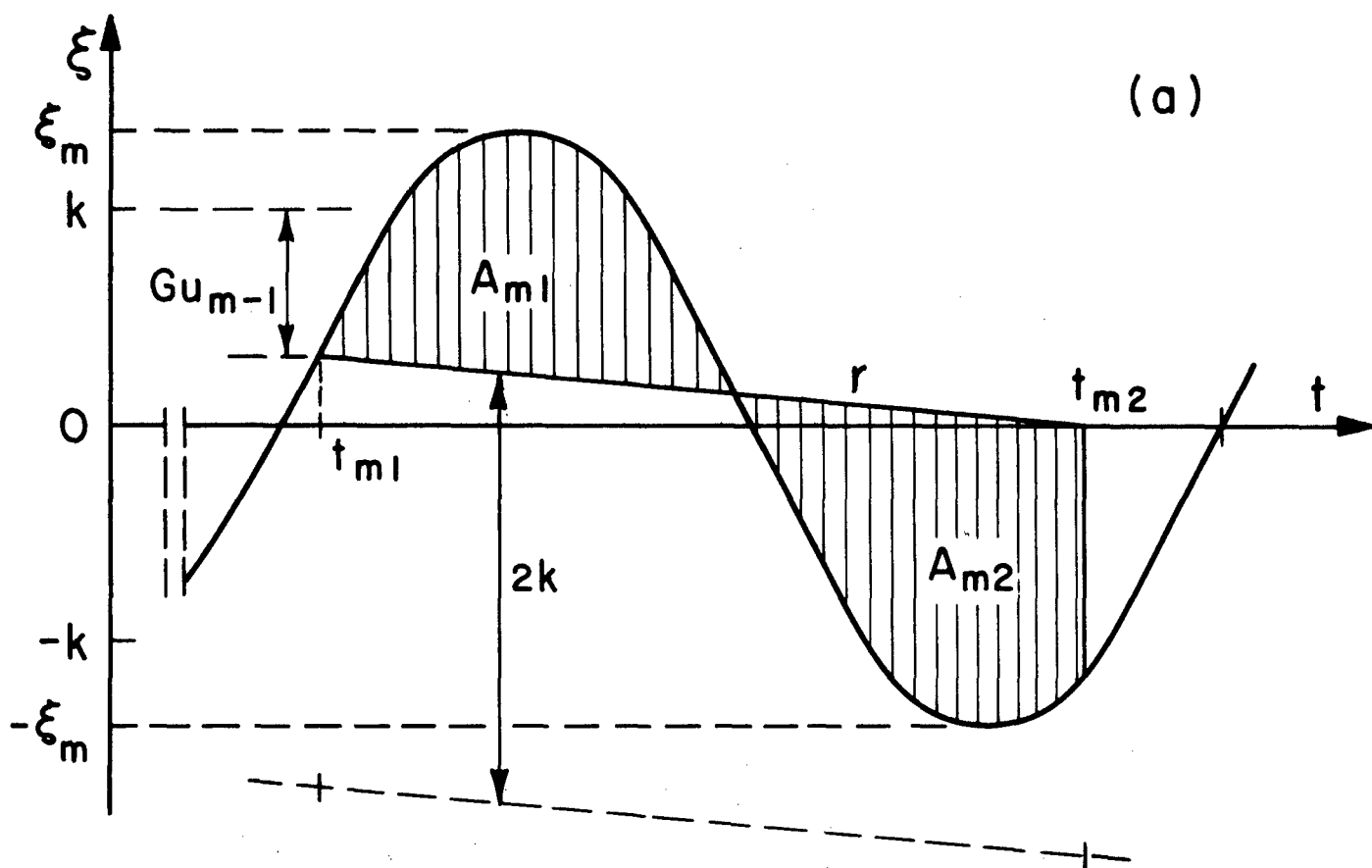


FIG. 4.6

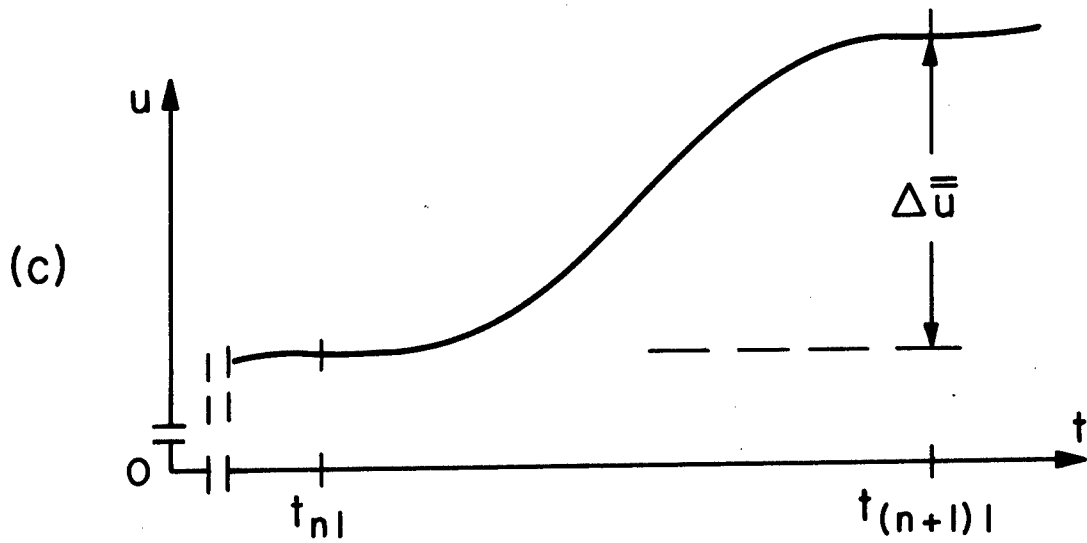
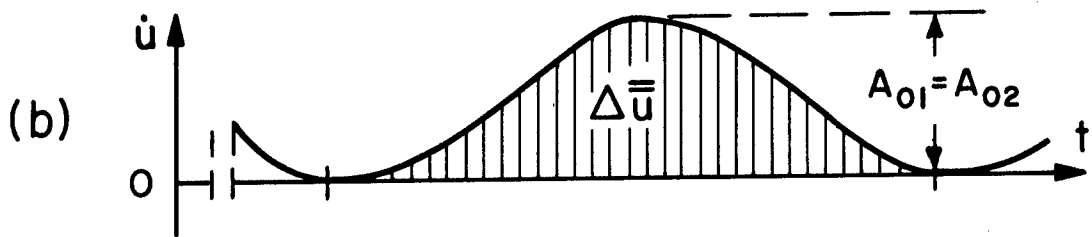
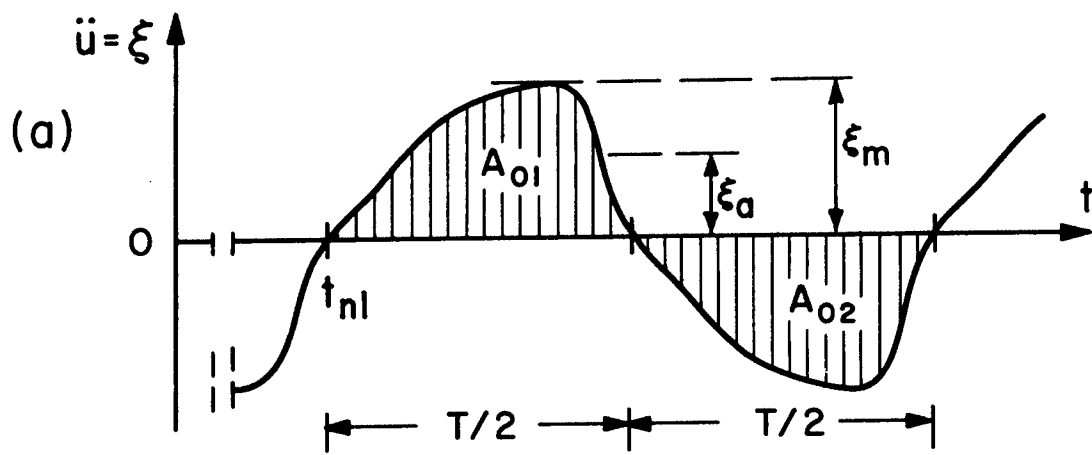


FIG. 4.7

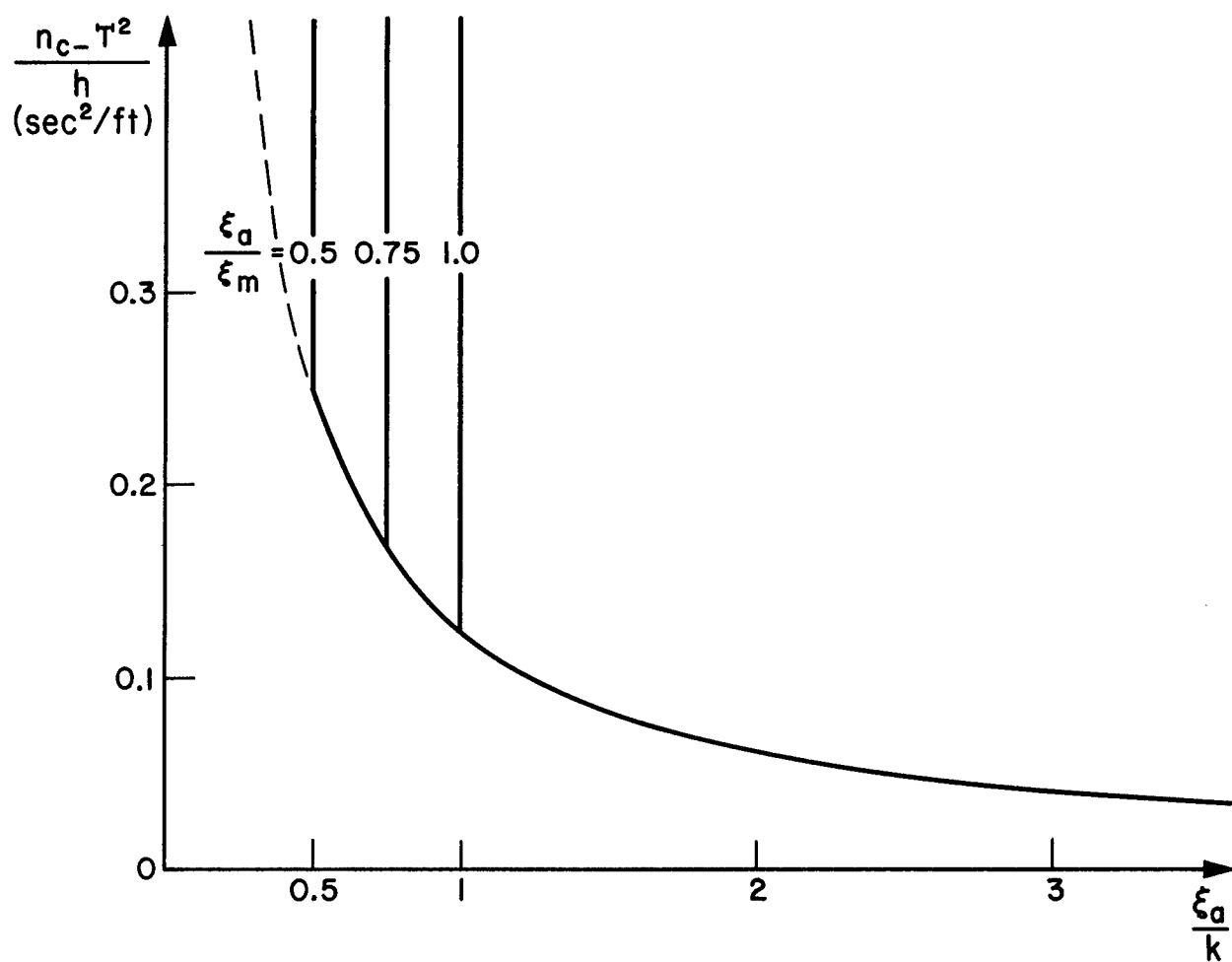


FIG. 4.8